PNNL-11628
UC-602

Pacific Northwest National Laboratory

Operated by Battelle for the
U.S. Department of Energy

Drying Behavior of K-East Canister Sludge

J. Abrefah
H. C. Buchanan
S. C. Marschman

May 1998

Prepared for the U.S. Department of Energy
under Contract DE-AC06-76RLO 1830

PNNL-11628

DISCLAIMER

PACIFIC NORTHWEST NATIONAL LABORATORY
operated by
BATTELLE
for the
UNITED STATES DEPARTMENT OF ENERGY
under Contract DE-AC06-76RLO 1830

Printed in the United States of America

Available to DOE and DOE contractors from the Office of Scientific and Technical Information, P.O. Box 62, Oak Ridge, TN 37831; prices available from (615) 576-8401.

Available to the public from the National Technical Information Service, U.S. Department of Commerce, 5285 Port Royal Rd., Springfield, VA 22161

This document was printed on recycled paper.
(9/97)

PNNL-11628
UC-602

Drying Behavior of K-East Canister Sludge

J. Abrefah
H. C. Buchanan
S. C. Marschman

May 1998

Prepared for
the U.S. Department of Energy
under Contract DE-AC06-76RLO 1830

Pacific Northwest National Laboratory
Richland, Washington 99352

Summary

A series of tests were conducted by Pacific Northwest National Laboratory to evaluate the drying behavior of sludge taken from the Hanford K-East Basin storage canisters. Some of the components of K-Basin sludge, such as oxides of uranium and its hydrates, could be associated with the spent nuclear fuel that will ultimately be loaded into Multi-Canister Overpacks (MCOs) and transferred to interim dry storage on the Hanford Site. The materials sealed in the MCOs must be compatible with the storage facility safety basis and the design accident analyses. Understanding the drying behavior of hydrates that may be formed by the reaction of uranium oxides (corrosion products) and water will help ensure these criteria are addressed.

Drying measurements of sludge samples collected from K-East Basin canisters showed the water content (physically[a] plus chemically[b] bound) to range between 5 wt% and 75 wt%. Uranium oxide hydrates, the main source of gaseous products that can pressurize the MCOs during storage, constituted about 3 wt% to 15 wt% of the total water content of the initial weight. Most of the physically bound water was assumed to be released from the samples at ambient temperature when the system was pumped down to vacuum conditions of about 40 mTorr. The period for release of most free water in the K-East canister sludge was about 24 hours.

Fourteen tests were run on subsamples from a batch of six larger K-East canister samples. The test temperatures ranged from ambient to about 625°C. For the last test, in which the drying was conducted in helium at atmospheric pressure, a partial loss of the physically bound water was observed before the start of the test. The complete release of the large fraction of free water remaining in the sample did not occur until the sample was heated to 75°C. This suggests that when a reasonable quantity of free water was present in the sample, the effective removal of the free water from the sludge occurred at temperatures equal to 75°C and above. This observation supports the assertion that most of the weight losses by the samples at temperatures below 75°C were caused by desorption of the remaining free water rather than by thermal decomposition of hydrates.

The thermal decomposition of the hydrates effectively started when the sample temperature was about 75°C. From the results of the test runs and analyses, thermal decomposition of the hydrates appears to drive the release of water, resulting in sample weight loss at temperatures between 75°C and

---

(a) Physically bound water is the "free water" that is physically absorbed by the pores and adsorbed by the surface of the sludge.

(b) Chemically bound water is the hydrate(s) and hydroxides formed by the reaction of water with the sludge; referred to here as "hydrates" or "hydrated species."

425°C. At temperatures above 425°C, the weight losses observed were due to reduction of higher oxides of uranium by reactions such as

$$3UO_3 = U_3O_8 + \frac{1}{2}O_2$$

rather than decomposition of hydrates.

The measured weight losses for the test temperature segments are listed in the table below.

Percent Weight Loss by K-East Canister Sludge

TGA Run	KE Sludge ID	Percent Weight Loss Based on Initial Sample Weight				
		RM to 50°C	50°C to 75°C	75°C to 300°C	300°C to 425°C	425°C to 625°C
31	96-05	0.38	0.23	0.71	NE	NE
32	96-05	0.06	0.34	0.28	NE	0.04
33	96-05	0.62	NE	0.29	0.05	0.02
36	96-01	0.19	0.13	3.03	1.20	0.16
37	96-01	0.18	0.12	1.62	0.31	0.25
38	98-08	NE	0.30	0.79	0.21	0.82
39	96-08	NE	NE	0.92	NE	NE
40	96-13	0.20	0.29	2.42	0.21	0.18
41	96-13	0.16	0.31	1.89	0.15	0.14
42	96-15	0.55	0.93	3.70	0.37	0.22
43	96-15	NE	0.20	3.36	0.23	0.18
44	96-08	0.22	0.22	3.04	0.38	0.29
45	96-04/L	0.63	2.30	10.4	1.50	0.69
46	96-08	7.74	1.44	4.08	0.62	0.31

TGA = thermogravimetric analysis; KE = K-East; ID = identification; RM = ambient temperature; NE = not evaluated.

The largest fraction of hydrated species thermally decomposed within the temperature range of 75°C to 300°C. The release rate curves (i.e., first derivative of the weight loss data) for this temperature range

exhibit characteristics similar to a multistep thermal decomposition reaction for the hydrate. Three reaction steps were identified from the release rate curve for the temperature range of 75°C to 300°C:

1. $UO_3 \cdot 2H_2O \rightarrow UO_3 \cdot H_2O + H_2O$

2. $UO_3 \cdot H_2O \rightarrow UO_3 \cdot 0.5H_2O + 0.5H_2O$

3. $UO_3 \cdot 0.5H_2O \rightarrow UO_3 + 0.5H_2O$

From these reaction steps it was proposed that the uranium trioxide hydrate, $UO_3 \cdot 2H_2O$, may be the hydrate material. This conclusion was supported by a positive identification of the $UO_3 \cdot 2H_2O$ phase by an X-ray diffraction analysis in two of the samples dried.

The three decomposition reactions were mechanistically represented by three release rate curves with peak temperatures of 147°C, 231°C, and 284°C for a temperature ramp of 1°C/min. These peak temperatures decreased with decreasing temperature ramp rate, indicating probable first-order decomposition kinetics. The experimental data for each deconvoluted peak was therefore fitted with a first-order kinetics equation using nonlinear regression. The fit yielded a reasonable rate constant for each of the three reaction steps. These test results and analyses indicate that most of the hydrated species present in the K-East Basin canister sludge will thermally decompose at temperatures below 400°C.

Acknowledgments

This work would not have been performed without the sampling of sludge from the storage canisters in the K-East Basin. The campaign to extract samples from the canisters was made possible through the dedicated efforts of the K-Basin operations staff and the DE&S Hanford, Inc., SNF characterization group under the management of Ronald Omberg and his associates, Bruce Makenas, Ronald Baker, and Leo Lawrence. The authors would also like to acknowledge the Radiochemical Processing Laboratory hot cell technicians, Pacific Northwest National Laboratory, who prepared the K-East canister sludge samples for the TGA testing. Finally, we thank Sue Gano for her editorial work and John Latkovich for his efforts in getting this report cleared and published.

Quality Assurance

This work was conducted under the Quality Assurance Program, Pacific Northwest National Laboratory (PNNL) SNF-70-001, *SNF Quality Assurance Program*, as implemented by the PNNL *SNF Characterization Project Operation Manual*. This QA program has been evaluated and determined to effectively implement the requirements of DOE/RW-0333P, Office of Civilian Radioactive Waste Management *Quality Assurance Requirements and Description* (*QARD*). Compliance with the QARD requirements is mandatory for projects which generate data used to support the development of a permanent High-Level Nuclear Waste repository. Further, the U.S. Department of Energy has determined that the testing activities which generated the results documented in this report shall comply with the QARD. Supporting records for the data in this report are located in the permanent PNNL SNF Characterization Project records, *Drying Behavior of K-East Canister Sludge*.

Contents

Figures

Tables

Acronyms

DSC	differential scanning calorimeter
ID	Identification
IPS	Integrated Process Strategy
KE	K-East
MCOs	Multi-Canister Overpacks
MS	mass spectrometer
NE	not evaluated
PNNL	Pacific Northwest National Laboratory
QA	quality assurance
QARD	Quality Assurance Requirements and Description
QMS	quadrupole mass spectrometer
RM	ambient temperature
SNF	spent nuclear fuel
TG	thermogravimetric
TGA	thermogravimetric analysis
XRD	X-ray diffraction

1.0 Introduction

Some corrosion products (sludge) generated during the storage of N-Reactor spent nuclear fuel (SNF) in the Hanford K-Basins will accompany SNF loaded into Multi-Canister Overpacks (MCOs) during implementation of the Integrated Process Strategy (IPS). The IPS was developed to package, dry, transport, and store the waste in an interim storage facility on the Hanford Site (WHC 1995). After treatment of the SNF before loading it into the MCOs, components of the corrosion materials (mainly oxides of uranium) will still be retained on some of the elements. The oxides of uranium will provide a large surface area for adsorption/absorption of water (physically bound) and will readily react with water to generate hydrates (chemically bound). The physically and chemically bound water will then be the primary source of gaseous products that can pressurize the MCOs. Water can also react with the exposed metallic uranium of damaged/corroded fuel elements to generate hydrogen during transport, staging, and storage. The IPS has process steps intended to dry the SNF to an expected product specification prior to sealing it in the MCOs. The drying behavior of the materials that will be sealed in the MCOs must be determined to ensure that the storage environment does not exceed the storage facility safety basis or design accident analyses. This report discusses a study conducted by Pacific Northwest National Laboratory (PNNL)[a] to evaluate the drying behavior of K-East Basin canister sludge, specifically the hydrated species.

A review of the literature indicated that two chemical phases of uranium oxide hydrates, uranium trioxide and uranium peroxide hydrates, can be formed by the reaction of water with uranium oxides. The uranium trioxide hydrates were identified in sludge samples taken from the storage canisters in the K-East Basin (Makenas et al. 1997) and in the sludge that accompanied a shipment of SNF samples from the K-West Basin (Abrefah et al. 1996). The uranium peroxide hydrates have been identified in surface coatings on SNF element samples from the K-East Basin and in some samples of sludge taken from the K-East floor (Makenas et al. 1996).

The formation of UO_3-based hydrates has been documented by Wheeler et al. (1964), Hoekstra and Siegel (1973), and Taylor et al. (1989). The thermal decompositions of the trioxide hydrates have been studied in detail by Wheeler et al. (1964) and Poko et al. (1968) and later reviewed by Hoekstra and Siegel (1973). The decomposition reactions reported involve the following steps:

1. Decomposition of the dihydrate, $UO_3 \cdot 2H_2O$, to the hydroxide, $UO_2(OH)_2$:

$$UO_3 \cdot 2H_2O \rightarrow UO_2(OH)_2$$
$$\sim 100°C < T < \sim 160°C$$

(a) Operated by Battelle for the U.S. Department of Energy under Contract DE-AC06-76RLO 1830.

2. Direct decomposition of $UO_2(OH)_2$ to UO_3:

$$UO_2(OH)_2 \rightarrow UO_3$$
$$\sim 250°C < T < \sim 260°C$$

3. Decomposition of $UO_2(OH)_2$ to $UO_3 \cdot 0.5H_2O$ followed by the decomposition reaction of $UO_3 \cdot 0.5H_2O$ to UO_3:

$$UO_3 \cdot 0.5H_2O \rightarrow UO_{3-x}$$
$$\sim 500°C < T < \sim 550°C$$

Two forms of the uranium peroxide hydrate are known: anhydrous peroxide, $UO_4 \cdot 4H_2O$ and dihydrate, $UO_4 \cdot 2H_2O$. Literature data on the thermal decomposition reaction of these hydrates date back to the 1800s. The dehydration process for $UO_4 \cdot 4H_2O$ has been studied by many researchers, including the 1922 study by Huttig and Schroeder reported by Katz and Rabinowitch (1951); Boggs and El-Chehabi (1957); Cordfunke (1961); Cordfunke and van der Giessen (1963); and Sato (1963). The first reaction is the decomposition of $UO_4 \cdot 4H_2O$ to $UO_4 \cdot 2H_2O$:

$$UO_4 \cdot 4H_2O \rightarrow UO_4 \cdot 2H_2O + 2H_2O$$
$$\sim 60°C < T < \sim 100°C$$

The dehydration is completed by thermal decomposition of $UO_4 \cdot 2H_2O$ to either X-ray amorphous or α-phase UO_3:

$$UO_4 \cdot 2H_2O \rightarrow UO_3 + \tfrac{1}{2}O_2 + 2H_2O$$
$$\sim 420°C < T < \sim 550°C$$

Based on these literature data, it appears a heat treatment scheme may be possible for removing water from hydrated species associated with oxides of uranium. A drying study of sludge collected from K-East storage canisters was performed by PNNL using a TGA/DSC/MS system (thermogravimetric analysis/differential scanning calorimeter/mass spectrometer). This report documents the drying results of 14 tests performed on K-East canister sludge samples and discusses analyses performed to determine the decomposition mechanisms of these materials.

A Netzsch STA 409 TGA/DSC/MS system was used to monitor the weight change of the samples due to weight loss (such as volatilization of water) when subjected to heating. The testing parameters (see Section 2.0) were selected to represent the IPS processing steps and did not represent those that would be selected for a detailed kinetic study of the drying behavior of the sludge. Volatilized species were monitored by the system's quadrupole mass spectrometer (QMS) for species identification. The tests were used to determine the relative amount of water in the samples and the fractional release of the moisture at certain desired temperatures.

2.0 Experimental

A schematic representation of the TGA/DSC/MS testing system is shown in Figure 2.1. The system is made up of four chambers: an MS chamber, an intermediate chamber, a sample reaction chamber, and a balance chamber. The MS chamber houses the QMS and is pumped by a turbomolecular pump to a baseline vacuum pressure of about 10^{-7} Torr. The intermediate chamber separates the MS chamber from the atmospheric reaction chamber and is pumped by a mechanical pump to a base pressure of about 10^{-3} Torr without a load.

The sample chamber is a tube (inside diameter of ~29 mm) and houses the thermogravimetric (TG) sample carrier. The TG sample carrier contains a bare-tip, S-type thermocouple that measures sample temperature. The TG sample carrier is connected to the analytical balance by a special "plug." Gas inlet and outlet lines are connected to the sample chamber to control the flow of reactant gas (if used). The sample chamber is resistively heated by graphite elements that are protected by a cover of ultra high purity helium gas flowing through the furnace shell. The analytical balance chamber houses the electrobalance. A gas inlet line is connected to the chamber so that the chamber can be purged with either an inert gas or the reactant gas. The temperature of the balance chamber is maintained at ambient conditions by a series of heat shields in the sample chamber and a water cooling crosshead at the joint that separates the balance chamber from the heated sample chamber.

The 14 K-East canister sludge subsamples used for the drying tests came from six out of the nine K-East canister sludge samples shipped to PNNL's Radiochemical Processing Laboratory (325 Building) hot cells for characterization. The sample crucibles, fabricated from alumina, measured 15 mm outside diameter, 12 mm inside diameter, and 7.2 mm deep, with an overall height of 9.0 mm. The average tare weight of the sample crucibles was about 2.6 g. Each crucible was mounted on top of an alumina head that was attached to the end of the TG sample carrier.

For each TGA run, about 80% volume of the alumina crucible was filled with a canister sludge subsample, weighed, and mounted on top of the TG sample carrier. The alumina crucible was covered with a perforated lid to prevent loss of the sample after drying. All the drying tests were performed under vacuum conditions with an ultra high purity helium background atmosphere, except TGA Runs 33 and 46, which were performed in helium at about 1 atmosphere system pressure (~760 Torr). The samples were dried over a temperature range of ambient to 625°C with thermal profiles like:

- Heat at a constant rate of 1°C/min to a temperature of about 50°C and hold at this temperature for 8 hours.
- Heat at a constant rate of 1°C/min to a temperature of about 75°C and hold at this temperature for 10 hours.

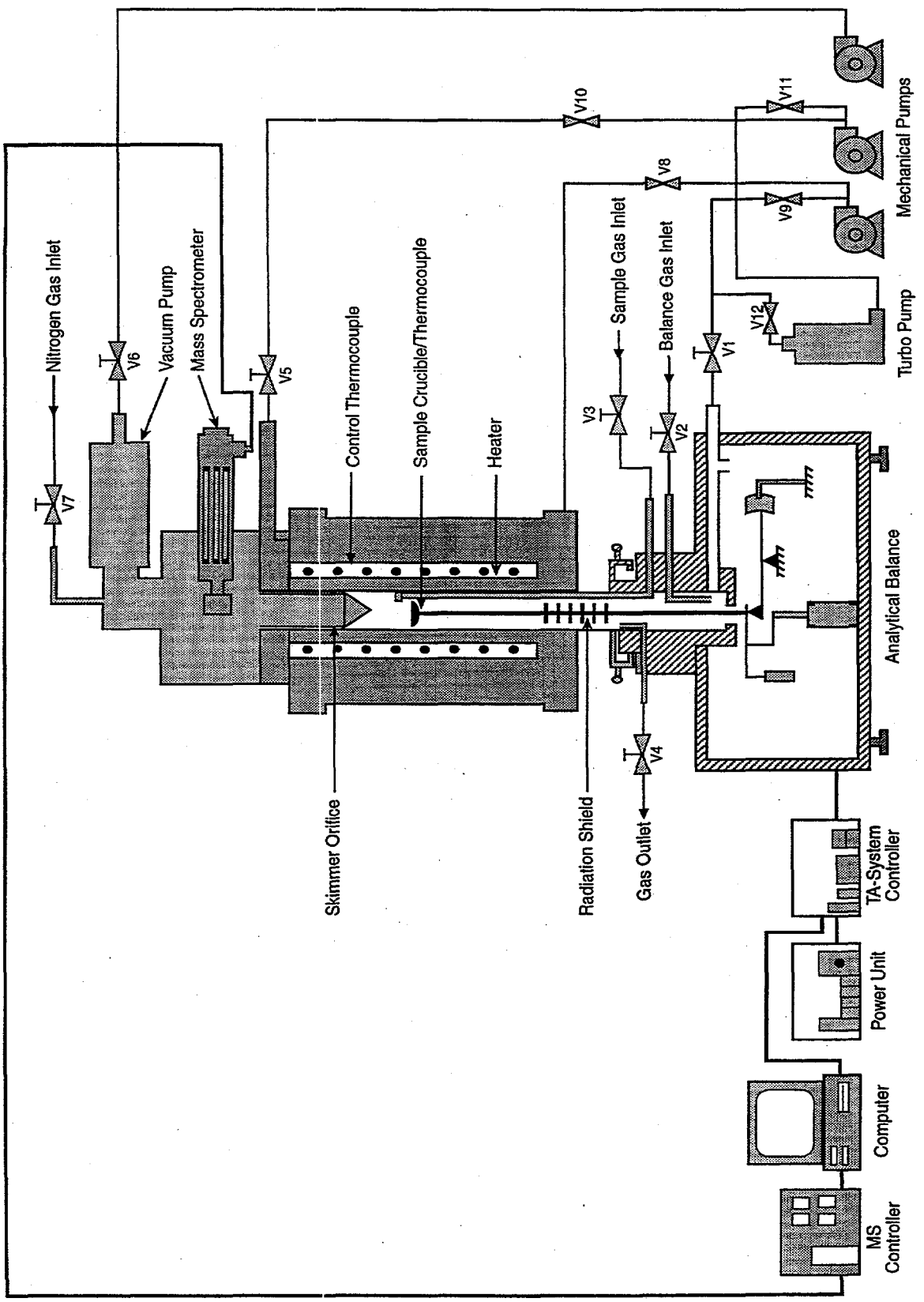

Figure 2.1. Schematic of the TGA/DSC/MS System

- Heat at a constant rate of either 1°C/min (Runs 33 through 42) or 0.2°C/min (Runs 43 through 46) to a temperature of about 300°C and hold at this temperature for 12 hours.

- Heat at a constant rate of 1°C/min to a temperature of about 425°C and hold at this temperature for 12 hours.

- Heat at a constant rate of 2°C/min to a temperature of about 625°C and hold at this temperature for 6 hours.

Once the heating steps above for TGA Runs 39, 42, 45, and 46 were completed, the samples were reheated to about 1000°C at a rate of 5°C/min to determine any additional release of volatile species (e.g., water) from the samples.

The TGA/DSC/MS system was initially evacuated to the lowest achievable vacuum (about 40 mTorr) at the start of each test. After evacuation, the vacuum pressure for each test was set by flowing ultra high purity helium gas through the sample chamber and throttling a valve to reduce the pumping speed of the sample environment. A helium flow rate of about 100 cc/min was needed to establish the test vacuum conditions. The actual partial pressure of water vapor in the system atmosphere was not measured but was likely less than or equal to the water impurity level in the ultra high purity helium. The gas supplier certificates showed that the water vapor impurity level in the ultra high purity helium was approximately 0.3 ppm. The water content of the helium gas in the system was lower for the last seven runs (40 through 46) because a molecular sieve purifier (specified to allow only parts per billion oxidants in the gas stream) was installed in the gas supply line.

The sample weight change was continuously monitored by the electrobalance throughout the test, and the off-gas stream was monitored by the QMS for the ions H^+, H^{2+}, OH^+, H_2O^+, O_2^+, and $^{137}Cs^+$. The weight lost by samples during the initial TGA/DSC/MS system evacuation was not recorded by the data acquisition system. Instead, the pre- and post-test weight measurements were used to determine the weight loss during this time period.

3.0 Drying Results

The TG results for the 14 drying tests are summarized in Table 3.1. Column 3 shows the system pressure conditions at the beginning of each test. Twelve tests were performed under a vacuum with a starting pressure in the range of 0.07 to 0.2 Torr, and two tests were conducted with the system near 1 atmosphere pressure. The sludge samples tested were taken from six out of nine larger K-East canister sludge samples, which are identified in Column 4. The pre- and post-test net weights of the test samples (as weighed on a balance separate from the TGA/DSC/MS system) are shown in Columns 5 and 6.

The total weight lost by each sample is shown in Column 7 of Table 3.1. These values represent the difference between the pre- and post-test weights (Columns 5 and 6). The total sample weight loss ranges from 62 mg (6% of the initial sample weight) for TGA Run 32 to 705 mg (77% of the initial sample weight) for TGA Run 38. Generally, all the samples taken from K-East canister sludge sample 96-08 (TGA Runs 38, 39, 44, and 46) showed higher weight loss. Visual examination showed those subsamples to appear damp as compared with the other subsamples. All the subsamples, with the exception of canister sludge subsample 96-04/Lower (TGA Run 45), had to be pumped for about 24 hours to release most of the free water (physically absorbed and adsorbed water molecules in/on the pores and surfaces of the sludge particles) prior to establishing the vacuum conditions of the tests.

The last five columns of Table 3.1 list the weight losses for the following five temperature segments of the test:

1. a ramp from ambient temperature to 50°C and a hold at 50°C for 8 to 10 hours (Column 8)
2. a ramp from 50°C to 75°C and a hold at 75°C for 10 hours (Column 9)
3. a ramp from 75°C to 300°C and a hold at 300°C for 10 to 12 hours (Column 10)
4. a ramp from 300°C to 425°C and a hold at 425°C for 10 to 12 hours (Column 11)
5. a ramp from 425°C to 625°C and a hold at 625°C for 6 to 8 hours (Column 12).

The NE (not evaluated) values shown in the table (TGA Runs 31, 32, 33, 38, 39) indicate that a weight loss was not detectable within the noise level of the electrobalance and/or a sample showed a weight gain due to oxidation reactions of some reactive component within a sample with background water vapor or oxygen. This difficulty in testing was solved when small leaks in the TGA/DSC/MS system were found and fixed, and a molecular sieve filter was installed in the helium gas supply line to remove water and oxygen impurities from the gas. Thus, for TGA Runs 40 through 46, the oxidation reaction interference with the weight loss data was negligible and could be discounted in the subsequent analyses of the data for those runs.

For most of the runs, the weight lost by a sample during a run (i.e., addition of the weight loss shown in the last five columns) was a small fraction of the total weight loss (Column 7).

Table 3.1. Drying Results of K-East Canister Sludge in Vacuum and in Helium at 1 Atmosphere

Run #		System Pressure (mTorr)[a]	Sample Characteristics				Weight Loss (mg) for Different Temperature Ranges (°C)				
TGA	K-East Sludge		ID	Pre-Test Weight (mg)	Post-Test Weight (mg)	Weight Loss (mg)	RM to 50	50 to 75	75 to 300	300 to 425	425 to 625
31	1	181	96-05	1384	1123	261	3.915	3.163	9.759	NE[b]	NE
32	2	93	96-05	1017	955	62	0.569	3.470	2.846	NE	0.434
33	3	~760x10³[b]	96-05	1000	836	64	6.216	NE	2.892	0.542	0.229
36	4	71	96-01	643	534	109	1.215	0.843	19.503	7.700	1.054
37	5	121	96-01	1054	860	194	1.898	1.265	17.078	3.268	2.635
38	6	70	96-08	917	212	705	NE	2.754	7.283	1.948	7.519
39	7	104	96-08	734	524	210	NE	NE	6.755	NE	NE
40	8	106	96-13	1159	986	173	2.369	3.313	28.080	2.475	2.041
41	9	125	96-13	768	654	114	1.265	2.349	14.548	1.175	1.084
42	10	96	96-15	723	603	120	3.976	6.690	26.744	2.711	1.626
43	11	132	96-15	1108	984	124	NE	2.169	37.23	2.530	1.987
44	12	90	96-08	1004	322	682	2.169	2.169	30.54	3.795	2.892
45	13	140	96-04/L	471	358	113	2.982	10.84	48.80	7.048	3.253
46	14	~760x10³[b]	96-08	771	440	331	59.71	11.11	31.49	4.800	2.390

ID = identification; RM = ambient temperature; NE= not evaluated.
(a) Starting pressures of the runs; and during the tests, the system pressure increased slightly due to increasing temperature.
(b) The system was at ambient pressure (i.e., about 1 atmosphere), and the actual pressure was not accurately measured.

Most of the observed weight loss in the last five columns can be attributed to the thermal decomposition of hydrated species, with interference from free water in the lower temperature segment (ambient to 50°C), and possibly to oxygen release due to decomposition of phases at temperatures above 425°C. The difference between the weight loss measured post-test (Column 7) and that determined to be lost during the heating cycles (the sum of the last five columns) was attributed to the removal of free water. An exception to this observation was the TGA Run 45 sludge subsample (taken from canister sample 96-04/Lower), which showed more than 50% of the weight loss was due to decomposition of hydrated species. The hydrated water accounts for between 4 wt% and 16 wt% of the subsamples, with subsample 96-04/Lower having the highest hydrate content. The 96-04/Lower was analyzed by X-ray diffraction (XRD) and found to contain a high content of schoepite ($UO_3 \cdot 2H_2O$, Figure B.1 in Appendix B).

Table 3.2 shows the detailed breakdown of the weight losses for each of the 10 temperature segments of the test. These weight losses will be used in Section 4.0 to deconvolute the total weight loss into three regions for mechanistic analysis of the data.

All the drying data indicate that most of the hydrated species decomposed during the temperature segment of 75°C to 300°C. The exception is TGA Run 46, but a comparison of the results of TGA Run 44 (canister sludge sample 96-08 in a vacuum) and TGA Run 46 (canister sludge sample 96-08 in flowing helium at atmospheric pressure) suggests that most of the water released in TGA Run 46 within the temperature range of ambient to 75°C was due to free water. The continued evolution of free water beyond the 50°C drying (in a flowing gas) period of about 10 hours indicates that all free water removal from the sludge occurred at temperatures greater than 50°C; and in TGA Run 46, the fraction of free water released at 75°C was significant enough to affect the analysis of the hydrate decomposition at that temperature.

The characteristics of the thermal decomposition of the hydrate(s) for the last seven runs (40 through 46) are shown in Figures 3.1 through 3.7. Figures for the first seven runs are shown in Appendix A. For each run, the weight change and the MS data for a mass/charge ratio of 18 (water) are plotted. For most of the runs, the plot of the MS data was comparable to the background signal, and quantitative analysis of the MS data for water released was not performed. The MS data must be treated as qualitative, but do show H_2O as the main species released. All the runs show considerably less, if any, interference from oxidation or absorption of water in the system than observed in the first seven runs (Appendix A) of the 14-run series. Again, this is due to addition of a chemical filter to the system background gas supply (helium) that reduced water and oxygen impurities in the background gas.

In Figure 3.1 (TGA Run 40), the weight change curve shows a small weight loss between ambient temperature and 50°C followed by a weight loss within the temperature range of 50°C to 75°C. At the end of each of these temperature segments, the weight change curve still shows decreasing behavior (i.e., a non-zero slope), which can be attributed to the slow decomposition of hydrated phases at these low temperatures.

Table 3.2. Drying Results of the Last Seven K-East Canister Sludge Samples

	Sample		Sample Weight Loss (mg) for Different Temperature Ranges									
TGA Run	ID	Weight (mg)	RM to 50°C	Held at 50°C	50°C to 75°C	Held at 75°C	75°C to 300°C	Held at 300°C	300°C to 425°C	Held at 425°C	425°C to 625°C	Held at 625°C
40	96-13	1159	0.67	1.70	0.18	3.13	20.83	7.25	1.55	0.93	1.19	0.85
41	96-13	768	0.23	1.04	0.25	2.10	11.80	2.75	0.64	0.54	0.59	0.49
42	96-15	723	0.65	3.33	0.64	6.05	22.18	4.56	1.93	0.78	0.89	0.75
43	96-15	1108	NE	NE	1.52	0.65	33.39	3.84	0.53	2.00	0.99	1.0
44	96-08	1004	0.94	1.23	0.01	2.16	28.02	2.52	2.31	1.49	2.16	0.73
45	96-04/L	471	0.32	2.66	1.60	9.24	44.70	4.10	4.63	2.42	1.76	1.49
46	96-08	771	9.87	49.84	1.55	9.56	28.31	3.18	2.18	2.62	1.22	1.17

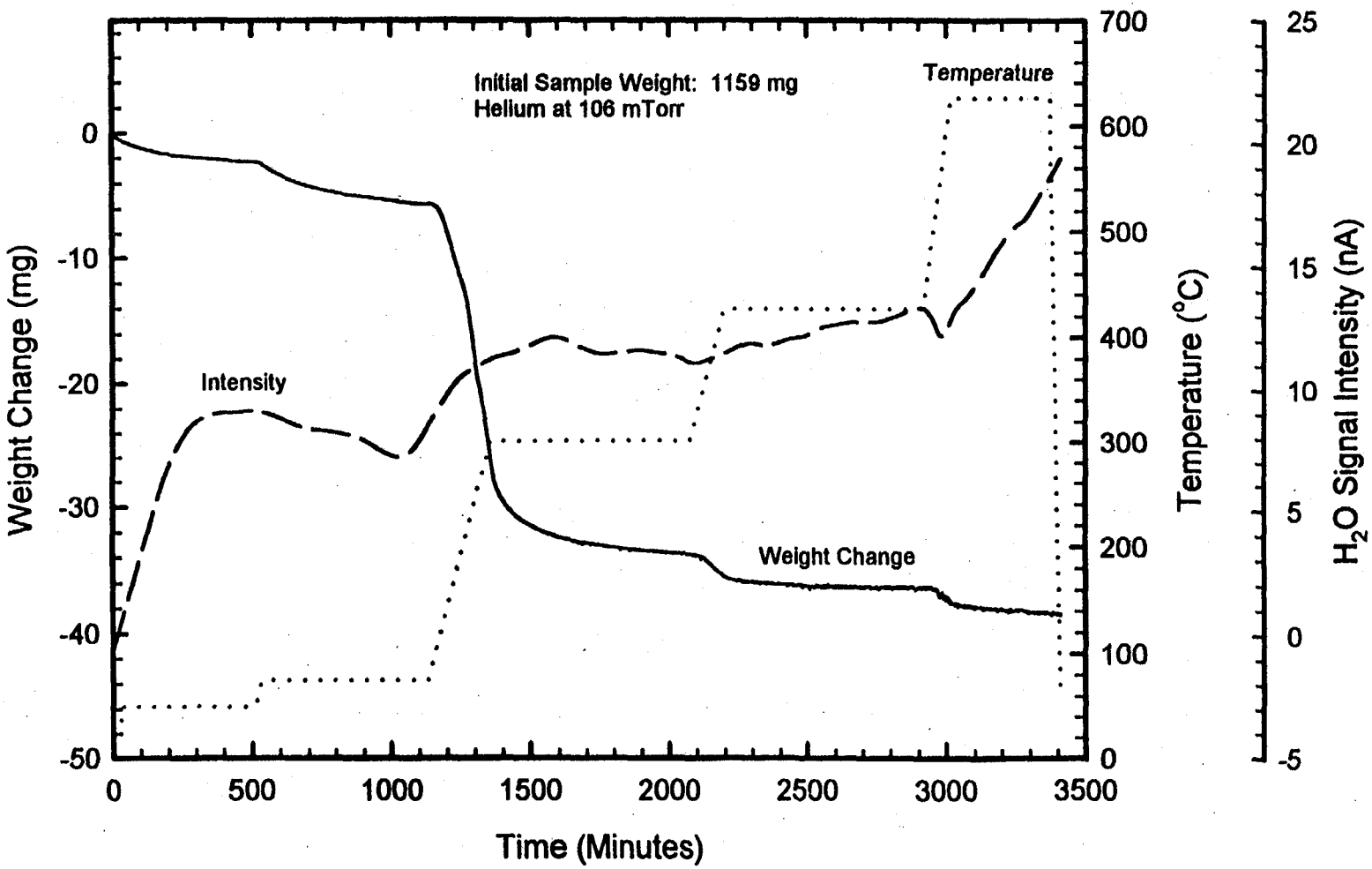

Figure 3.1. TGA Run 40 Plot Showing Weight Change, MS Signal for H_2O, and Temperature Versus Time for K-East Canister Sludge 96-13

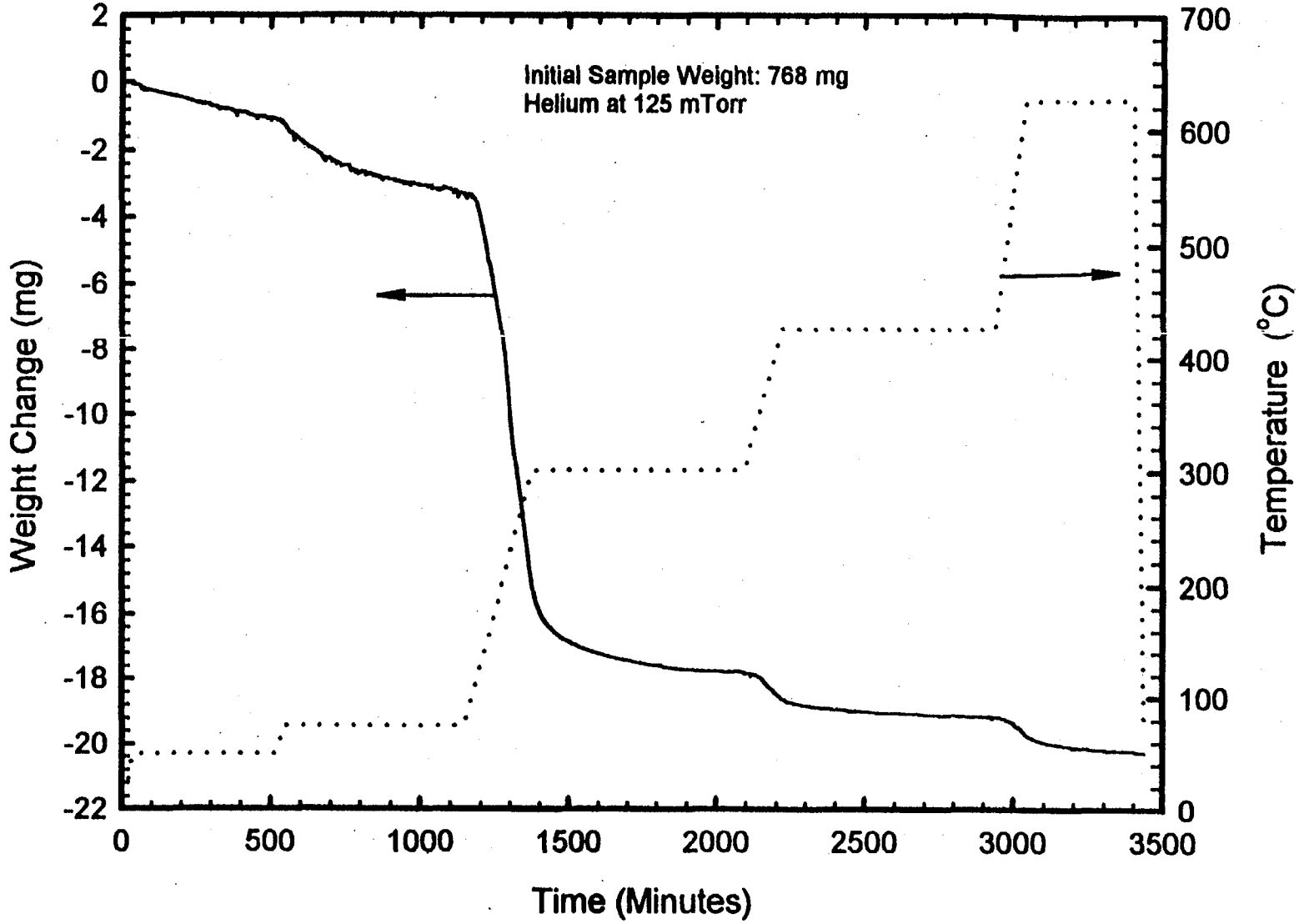

Figure 3.2. TGA Run 41 Plot Showing Weight Change, MS Signal for H_2O, and Temperature Versus Time for K-East Canister Sludge 96-13

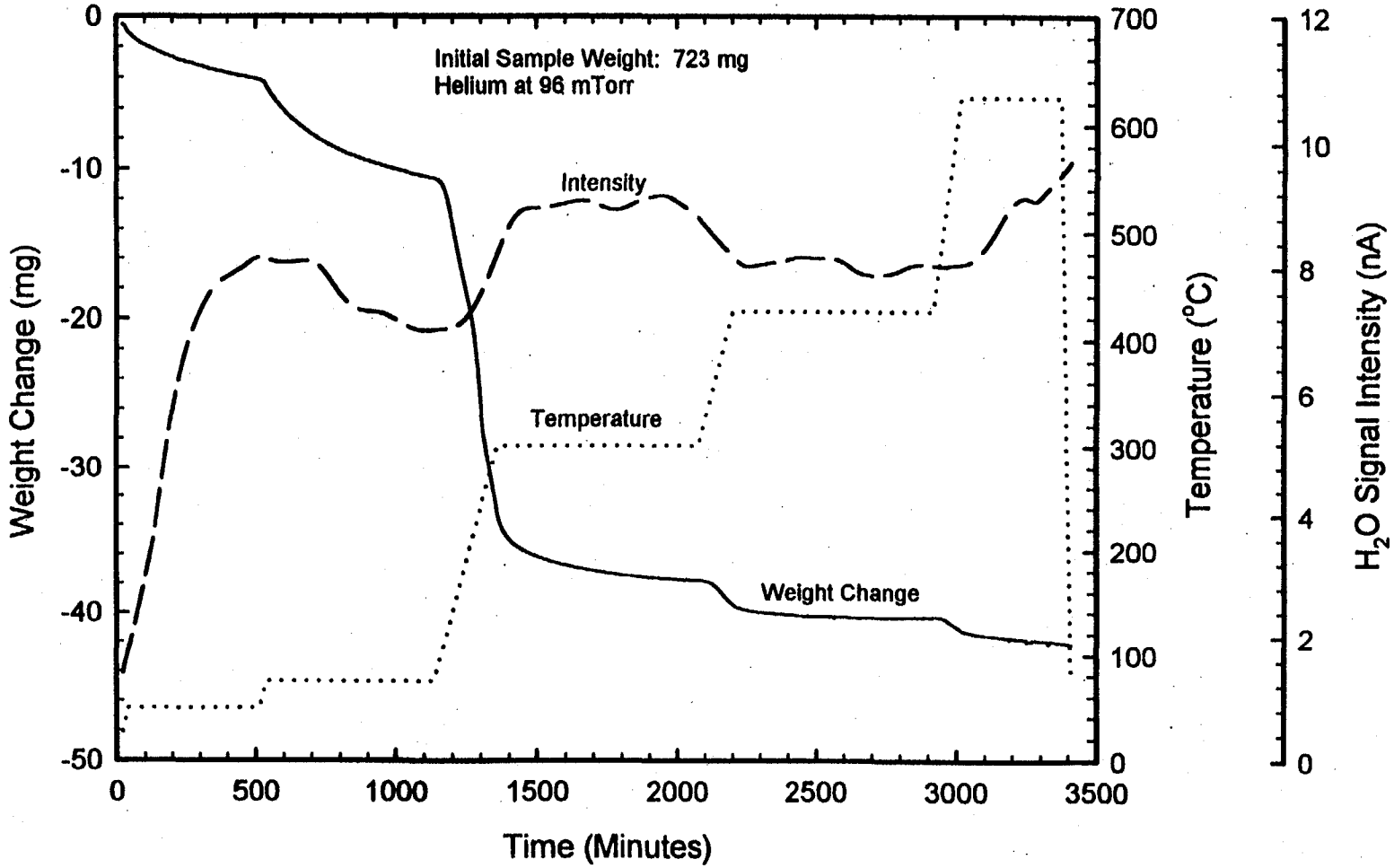

Figure 3.3. TGA Run 42 Plot Showing Weight Change, MS Signal for H_2O, and Temperature Versus Time for K-East Canister Sludge 96-15

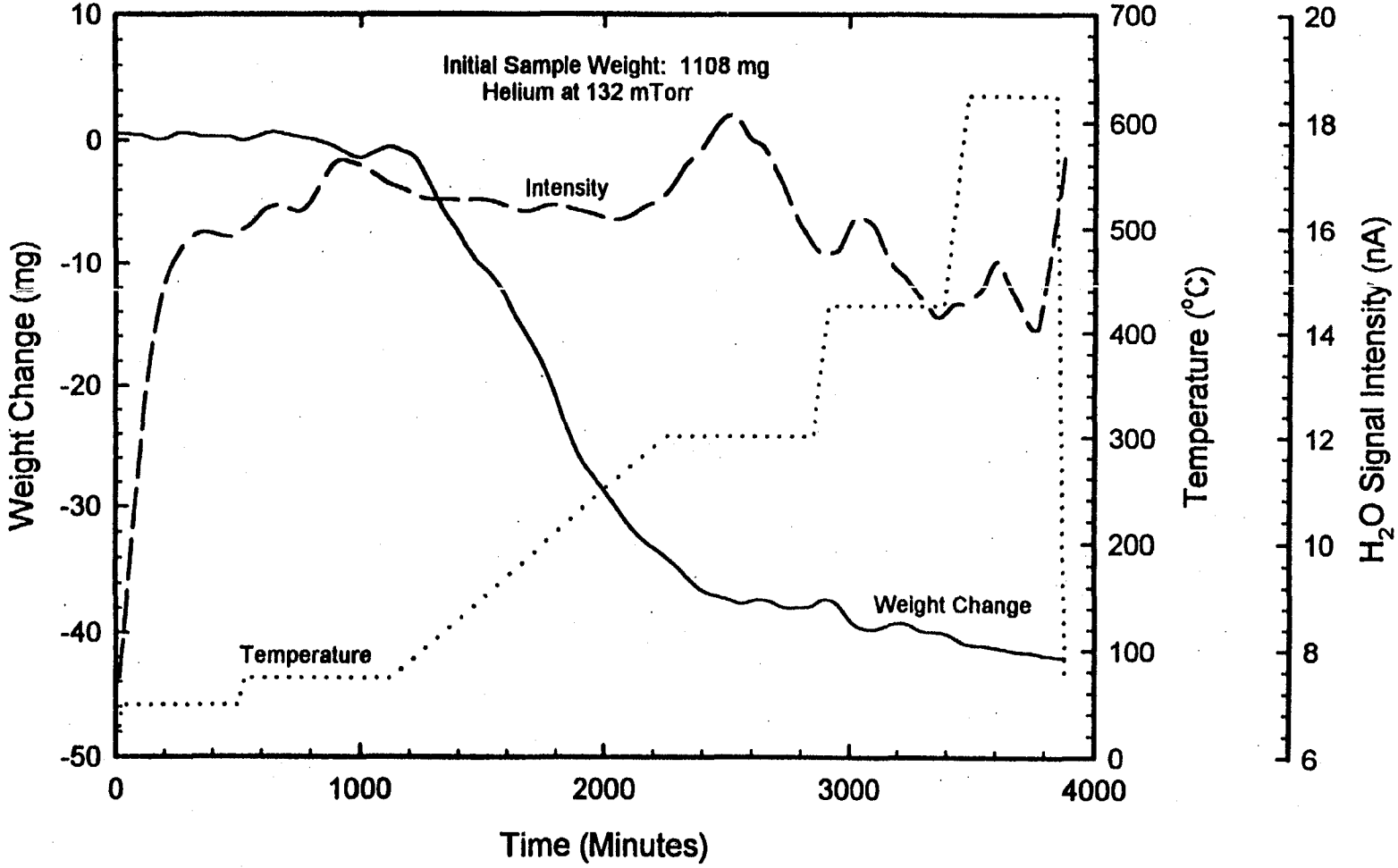

Figure 3.4. TGA Run 43 Plot Showing Weight Change, MS Signal for H_2O, and Temperature Versus Time for K-East Canister Sludge 96-15

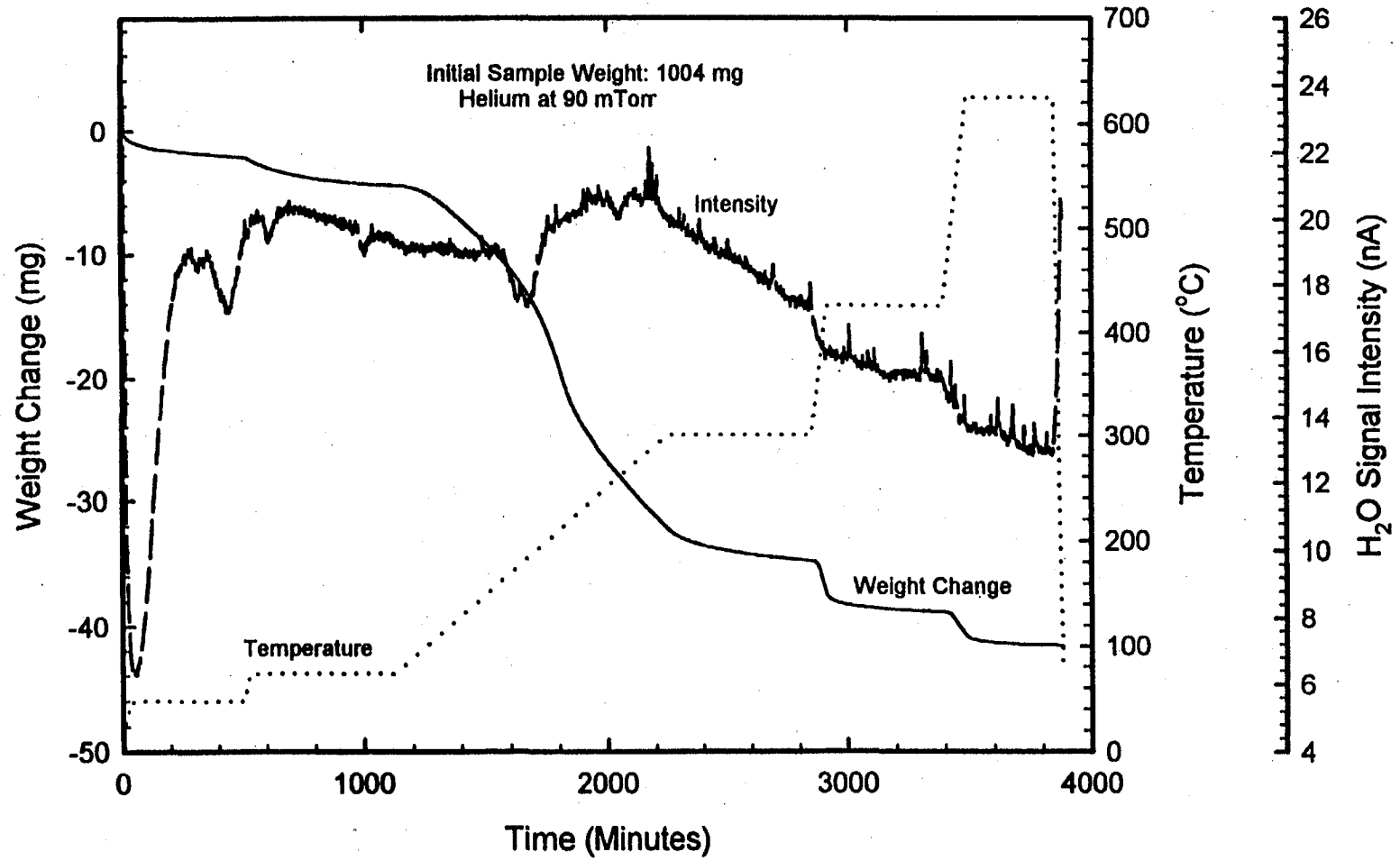

Figure 3.5. TGA Run 44 Plot Showing Weight Change, MS Signal for H_2O, and Temperature Versus Time for K-East Canister Sludge 96-08

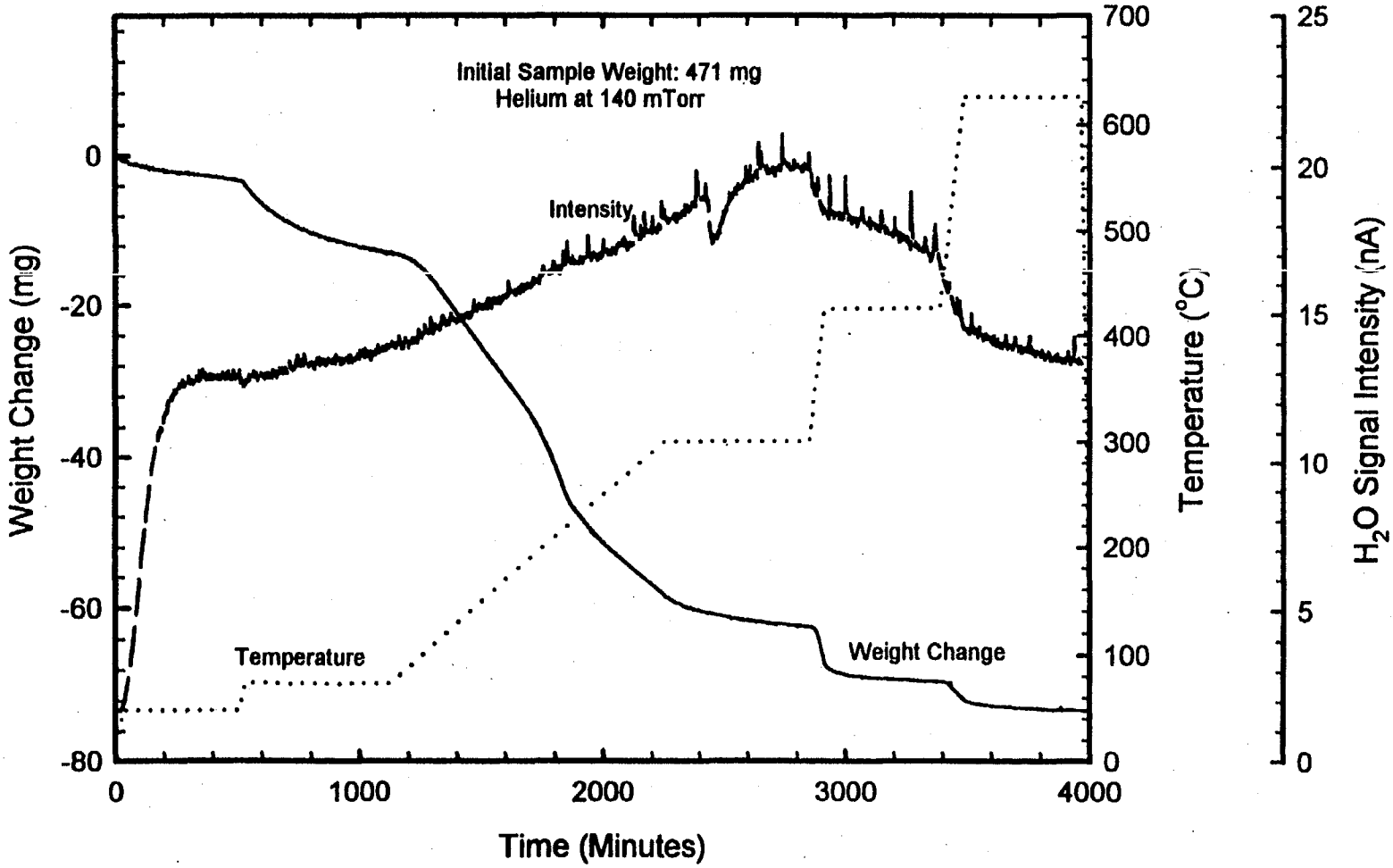

Figure 3.6. TGA Run 45 Plot Showing Weight Change, MS Signal for H_2O, and Temperature Versus Time for K-East Canister Sludge 96-04/Lower

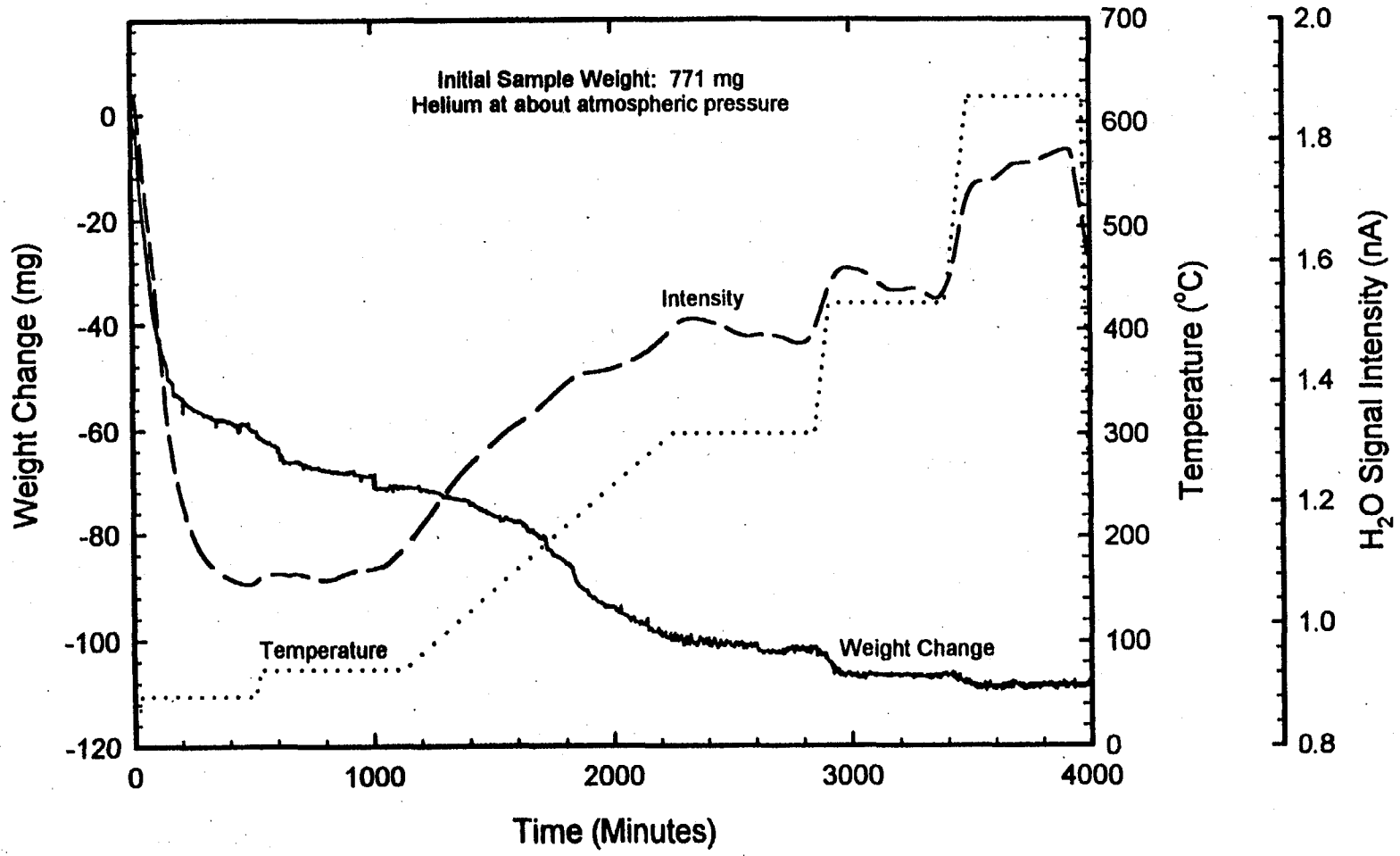

Figure 3.7. TGA Run 46 Plot Showing Weight Change, MS Signal for H_2O, and Temperature Versus Time for K-East Canister Sludge 96-08

The weight loss measured within the next temperature range (75°C to 300°C) is the largest, and there is an indication of a slope change for the weight change curve at about 219°C. The slope change of the weight loss indicates more than one type of hydrated phase may be releasing water. If it is assumed that only one hydrated phase exists at the start of drying, then the slope changes can be used to determine the thermal decomposition of that particular hydrated phase in the sludge sample. The sample for this run showed small weight losses at temperature ranges of 300°C to 425°C and 425°C to 625°C. The total weight loss measured at temperatures above ambient was 3.3 wt% of the initial sample weight. Overall, this sample lost a total of about 15 wt% of its initial weight, which is about 11.7 wt% physically absorbed and adsorbed water (water removed at ambient temperature during a system pumpdown) and 3.3 wt% chemically bound water (water released during heating). The data obtained from the MS showed water was released over the heating cycle; however, the background "noise" level was high enough to make any quantitative estimate invalid.

Figure 3.2 shows the drying results of TGA Run 41. During this run the MS was not functional (filament failure), and only the weight change data can be reported. The sample lost significant weight between 75°C and 300°C, and had measurable weight losses within the temperature ranges of ambient to 50°C, 50°C to 75°C, 300°C to 425°C, and 425°C to 625°C. A continuous decrease in weight at the two lower temperature segments was observed in this run similar to TGA Run 40. The weight loss between 75°C and 300°C also showed a change in slope, indicating different hydrated species being released by the sample. The total weight loss of this run was also about 15 wt%, and the fractional weight loss at temperatures above ambient was 2.7 wt%. If the latter is assumed to be due to thermal decomposition of hydrated species, the physically absorbed and adsorbed water corresponds to about 12.3 wt%. The samples for TGA Runs 40 and 41 came from the same canister, and the difference in the hydrated fraction in both runs may be an indication that not all the sludge is in a hydrated form. Thus, any tests that use only a small portion of the sample can be biased.

Figure 3.3 shows the data from TGA Run 42. The weight-loss curve is very similar to TGA Runs 40 and 41. Small weight losses occurred within temperature ranges of ambient to 50°C and 50°C to 75°C. A significant weight loss was measured between 75°C and 300°C. The sample showed slight weight decreases within the temperature ranges of 300°C to 425°C and 425°C to 625°C. The MS signal for this run suffered from a high background signal that prevented quantitative analysis of the water signal corresponding to the weight losses.

The results of TGA Run 43 (illustrated in Figure 3.4) showed a very small weight loss at temperatures below 50°C, which was difficult to evaluate given the system noise level during the measurement. The weight loss in the temperature range 50°C to 75°C was again small but was measurable and could be evaluated. The most significant weight loss occurred within the temperature range of 75°C to 300°C. The majority of the weight loss for this temperature range occurred during the ramp from 75°C up to 300°C (a total time of about 19 hours). The sample lost about 4 mg (of the total weight loss of 37.2 mg) for that temperature range at the isothermal period of 10 hours at 300°C. The weight losses within the temperature ranges 300°C to 425°C and 425°C to 625°C were also small but measurable. The MS signal in the figure shows a high background signal level, which again makes it very difficult to differentiate the water signal resulting from the sample drying.

In Figure 3.5, TGA Run 44, the weight change curve shows a small weight loss between ambient temperature and 50°C, followed by yet another small weight loss within the temperature range of 50°C to 75°C. The last portion of the weight change curve for each of these temperature segments (ambient to 50°C, 50°C to 75°C) still shows decreasing behavior (i.e., a non-zero slope) at the end of the prescribed hold period. This incomplete release of moisture at these two temperature segments may be due to the slow decomposition of the higher temperature hydrate(s) at these low temperatures and test pressures. The weight loss measured within the next temperature range (75°C to 300°C) is the largest, and there is an indication of a slope decrease for the weight change curve. The decreasing slope indicates an increasing water release rate by the sample or a change in the release rate mechanism. The sample for this run showed small weight losses over the temperature ranges of 300°C to 425°C and 425°C to 625°C. The total weight loss measured at temperatures above ambient was 4.2 wt% of the initial sample weight. Overall, this sample lost 66 wt% of its initial weight, of which 61.8 wt% was physically absorbed and adsorbed water and 4.2 wt% chemically bound water. The MS signal curve (curve smoothed using Lorentz method to remove the signal noise) indicated water was the volatile product released within the temperature ranges considered, but the noise and background signal levels were high enough to invalidate any quantitative estimates.

Figure 3.6 shows the drying results of TGA Run 45. The sample lost significant weight between 75°C and 300°C, and small weight losses occurred within the temperature ranges of ambient to 50°C, 50°C to 75°C, 300°C to 425°C, and 425°C to 625°C. However, the weight loss over the temperature range of 50°C to 75°C was higher than both the weight loss in the preceding temperature segment (ambient to 50°C for TGA Run 45) and the weight loss within the same temperature range (50°C to 75°C) for TGA Run 44. This increase in the weight loss may suggest an increase in the hydrate content of this sample relative to the previous sample, and also an increase in the thermal decomposition of the hydrate at temperatures above 50°C. The weight change curve also indicates a continuous decrease in weight close to the end portion of the two lower temperature segments. This observation supports the assertion that this may be due to thermal decomposition of the same hydrated species. The total weight loss of this run was about 24 wt%, and the fractional weight loss at temperatures above ambient was 15.5 wt%. Assuming the latter to be due to thermal decomposition of hydrated species, the physically absorbed and adsorbed water corresponds to approximately 8.5 wt%.

The weight-loss curve for TGA Run 46 is shown in Figure 3.7. This test was performed at about 1 atmosphere pressure. A significant weight loss was measured at temperatures below 50°C because the pre-test sample preparation did not remove all the free water. The weight loss over the temperature range of 50°C to 75°C was small compared to what was measured below 50°C but compared well with the measured weight loss for a similar sample (96-08 in TGA Run 44). The weight loss showed an increase of about a factor of 5. A significant weight loss was measured between 75°C and 300°C. A temperature of about 218°C corresponds to the point where the slope changes on this weight change curve occurred. The sample showed slight weight decreases within the temperature ranges of 300°C to 425°C and 425°C to 625°C. The MS signal for this run also suffered from a high background signal that prevented quantitative analysis of the water signal corresponding to the weight losses. Qualitatively, the MS signal indicated release of water from the sample during measured weight losses.

Two sludge samples were reheated to determine if additional weight changes might be observed at higher temperatures. The weight change data for reheating the sludge samples used in TGA Runs 42 and 45, up to 1000°C, are plotted in Figure 3.8. The figure indicates a decrease in the sample weight starting at about 645°C (reheat of TGA Run 42) and about 675°C (reheat of TGA Run 45) and continued to the end of the test. The slope for the decrease in weight changed when the sample temperature reached about 1000°C. The total weight loss was 3.05 mg (about 0.42 wt% of initial sample weight) for the reheated sample of TGA Run 42 and 6.26 mg (about 1.33 wt% of initial sample weight) for the reheated sample of TGA Run 45. The decrease in sample weight upon reheating indicates that the release of all volatile species (including thermal decomposition of water) was not complete during these runs. The weight loss may be due to a hydrate decomposition process or possibly the decomposition of UO_3 to U_3O_8 at higher temperatures, releasing oxygen.

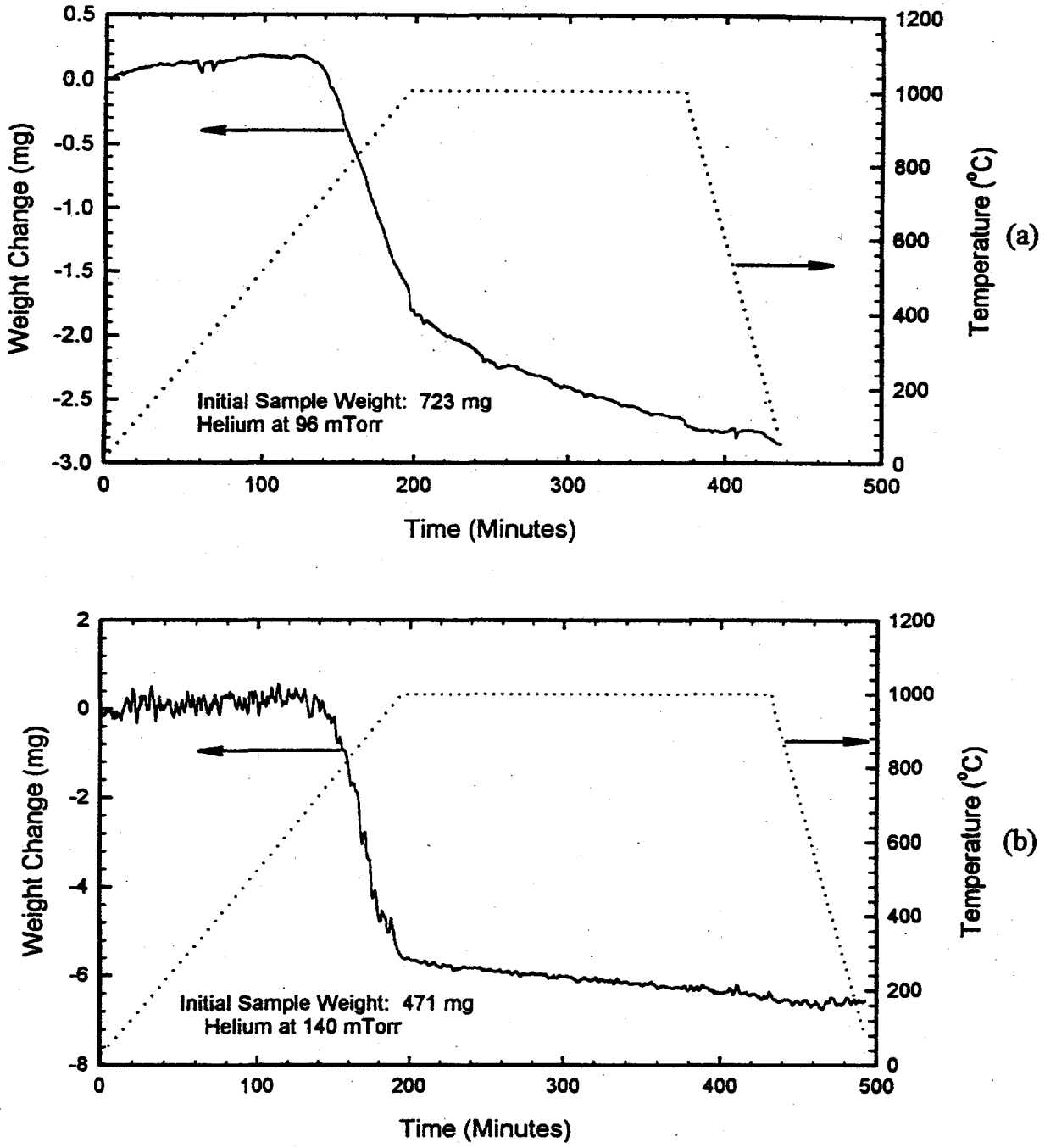

Figure 3.8. Plots Showing Weight Change and Temperature Versus Time for Reheating of K-East Canister Sludge Subsamples, (a) 96-15 After TGA Run 42 and (b) 96-04/Lower After TGA Run 45, to 1000°C

4.0 Drying Kinetics of K-East Canister Sludge

The K-East canister sludge dehydration results were analyzed to determine rate kinetics. The TGA weight loss data were first divided into three regions (discussed in Sections 4.1 through 4.3):

1. The weight loss from ambient temperature up to 75°C (Columns 4 through 6 of Table 3.3), which was due to desorption of physically bound water (free water) from the surfaces and the pores of the sludge particulates.

2. The weight loss from 75°C up to 425°C (Columns 7 through 10 of Table 3.3), which was due to thermal decomposition of hydrated species (i.e., chemically bound water).

3. The weight loss at 425°C and temperatures above (last three columns of Table 3.3), which was due to evolution of oxygen by the sludge sample. The evolving oxygen is due to reduction of uranium oxide to a lower oxygen/uranium ratio oxide such as:

$$3UO_3 \rightarrow U_3O_8 + \tfrac{1}{2}O_2$$

The actual weight loss data did not have precisely defined temperature boundaries, and there were interferences that influenced the data. For example, during TGA Run 46, the free water desorption was not complete until the sample was held at 75°C for 10 hours. Due to experimental difficulties (see Section 3.0), the results of the first seven runs (TGA Runs 31 through 33, 36 through 39) will not be included in these analyses.

4.1 Free Water Desorption Kinetics

The weight loss due to moisture release from K-East canister sludge samples from ambient temperature up to 75°C (i.e., not including the release at 75°C) can be attributed to the desorption of the remaining "free water" in the sludge. The total measured free water weight losses by the K-East canister sludge samples for the last seven runs are listed in the second column of Table 4.1. The free water lost before each test could not be determined. The free water lost during the system evacuation can be estimated from data shown in Table 3.1. These estimates range from 7 wt% (TGA Run 43) to 64 wt% (TGA Run 44). The free water released during the tests (Table 4.1) was a small fraction of the estimated initial free water content of the sludge samples, with the exception of TGA Run 46 where the measured value was about 22 wt% of the estimated free water weight. For TGA Runs 40 through 45, the measured free water fractions range between 1.5 wt% and 10 wt% of the total estimated free water content of the sludge samples. Thus, only small weight losses were measured for the temperature segments apportioned to free water desorption, with the majority occurring at the isothermal temperature of 50°C. Based on this information, only the weight loss at 50°C was analyzed to determine the free water desorption rate constant.

Table 4.1. Free Water Desorption Rate Constant at 50°C

TGA Run	Total Free Water[(a)] Loss (mg)	Weight Loss at 50°C (mg)	Desorption Rate Constant, k x 10^3 (min^{-1})	r^2 of the fit
40	2.55	1.70	4.72	0.99
41	1.52	1.05	2.88	0.98
42	4.62	3.33	3.49	1.0
44	2.18	1.23	5.29	0.92
45	4.58	2.66	1.80	0.98
46	61.3	49.8	10.5	0.98

(a) This is the free water left in the sample after drying the sample at ambient temperature in a vacuum for about 24 hours before the start of the test.

The weight loss kinetics of the sludge at 50°C was analyzed with the assumption of a single desorption site to estimate the desorption rate constant. There is the possibility of multiple sites for the free water; however, an effective single site desorption kinetics analysis may still be a good approximation, if the bond strengths of the multiple sites are not very different from each other.

The analysis was performed for TGA Runs 41 and 42 and 44 through 46. TGA Run 43 was excluded in the analysis because the data were insufficient. The total concentration of free water in each run was calculated by adding the weight loss for the temperature segments, RM (ambient) to 50°C, at 50°C, and 50°C to 75°C listed in Table 3.2. The weight loss at 50°C was then normalized by dividing the free water concentration by the total free water concentration. Results of the normalized data for TGA Runs 40 and 46 are shown in Figures 4.1a and 4.1b. By this normalization, it is implied in this analysis that the free water is uniformly dispersed in the sample. This assumption is valid given that the sample is made up of small particles, and the atmosphere surrounding each particle is considered linked to each other and provides no limitation for migration of the water molecule. The normalized weight loss data were fitted with a desorption kinetic equation:

$$df/dt = -k_f f \tag{4.1}$$

where f is the concentration of free water in the sludge, and $k_f = k_{f0}\exp(-Q_f/T)$ is the first-order rate constant with a pre-exponential factor, k_{f0} (min^{-1}), and activation energy, Q_f (K). At constant temperature, k_f in Equation (4.1) is constant and the equation can be solved to yield:

$$f/f_o = \exp(-k_f t) \tag{4.2}$$

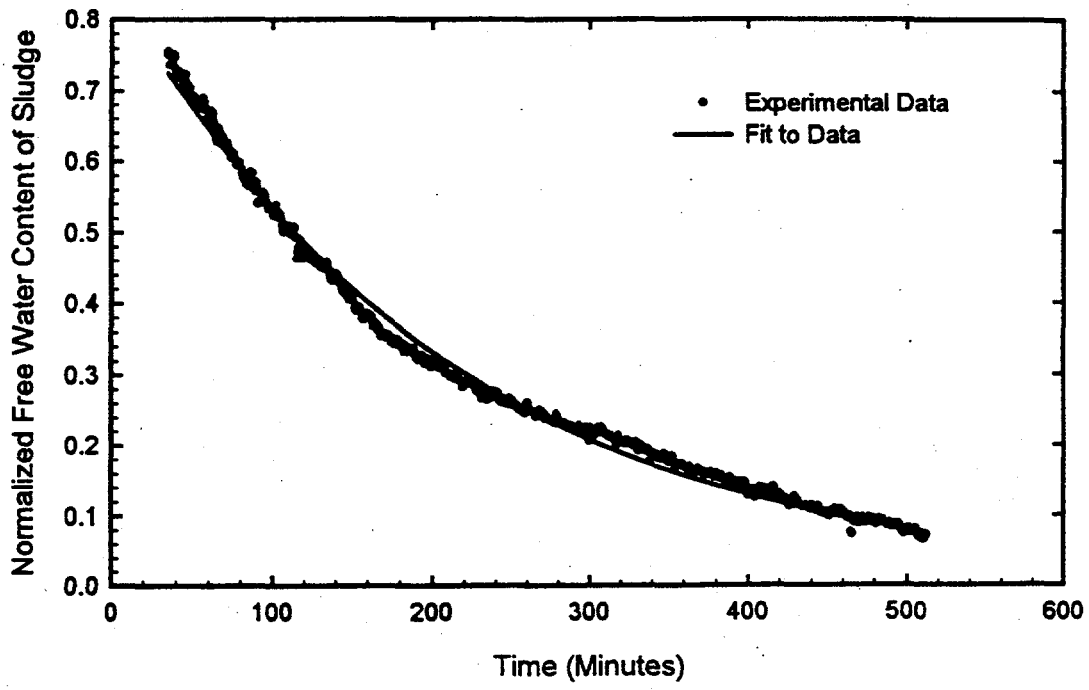

(a)

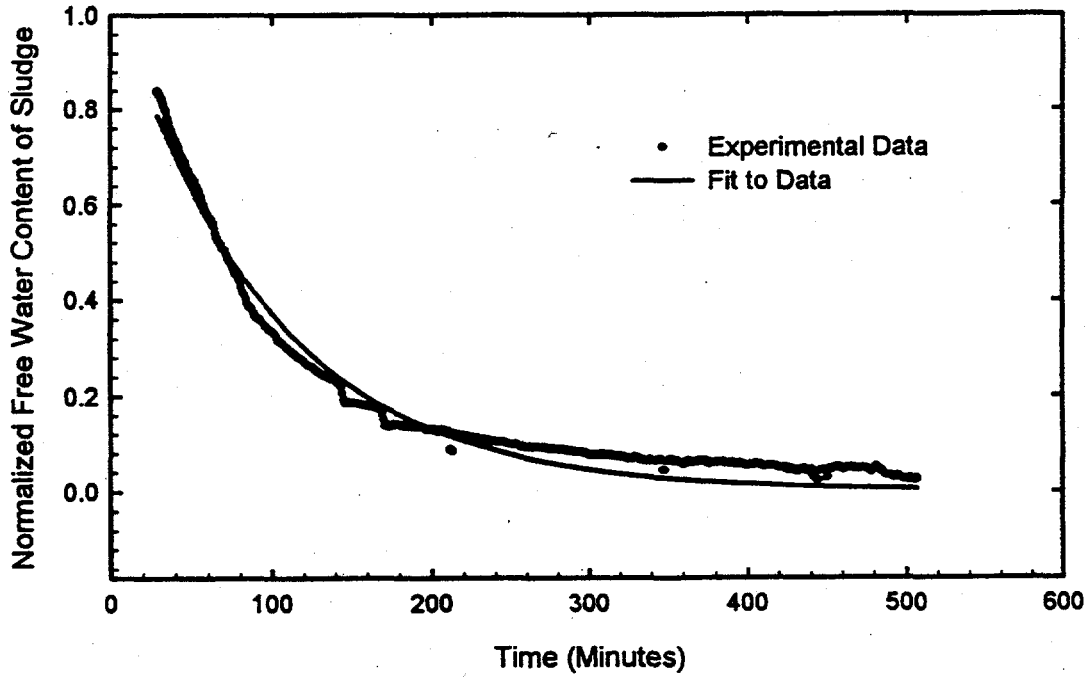

(b)

Figure 4.1. Plots of a Theoretical Fit to the Isothermal Data at 50°C (a) TGA Run 40 and (b) TGA Run 46

where f_0 is the free water concentration in mg at zero time. A nonlinear fit of the normalized experimental data at 50°C using Equation (4.2) with k as the only fitting parameter was computed to obtain values of k at 50°C. Table 4.1 shows the desorption rate constant for the six TGA runs analyzed. The fitted curves for TGA Runs 40 and 46 are shown as solid lines in Figure 4.1.

The averaged rate constant for the free water desorption is 4.8×10^{-3} min^{-1}. This indicates that the averaged first-order-kinetics half life, τ, for desorption of free water from the K-East canister sludge, is about 2.4 hours, which implies that (for the K-East canister sludge tested) it takes about 24 hours (10τ) to remove about 99.9% of the free water. This rate then explains why the 10-hour 50°C isothermal drying time used in TGA Run 46 was insufficient to remove the free water and this water was not completely removed until the sample was heated to 75°C.

4.2 Hydrate Thermal Decomposition Kinetics

The thermal decomposition of hydrated species in the K-East canister sludge is assumed (in the data analysis) to occur over the temperature range of 75°C up to 425°C (excluding the weight loss at 425°C). The weight loss data for this temperature range (75°C to 425°C) are listed in Columns 7 through 10 of Table 3.2. Two mechanistic approaches were considered in analyzing the thermal decomposition kinetics of the hydrates:

1. A hydrated species with one-step thermal decomposition reaction such as

$$UO_x \cdot yH_2O \rightarrow UO_x + yH_2O \tag{4.3}$$

2. A hydrated species with a multiple step thermal decomposition.

The data collected over the dehydration temperature range included two isothermal segments. These isothermal segments were at 75°C and 300°C for a period of about 10 hours. Depending on the mechanism used, the data at these isothermal conditions required different normalization schemes. Even though the bulk of the dehydration analysis included the two mechanistic approaches, the multiple step kinetics at 75°C has been included in this report.

4.2.1 Dehydration Kinetics at 75°C

The isothermal decomposition of the hydrate at 75°C was analyzed by assuming first-order decomposition kinetics. The weight loss data at 75°C were adjusted such that hydrate released was a fractional part of the first decomposition step for a multistep release mechanism that will be discussed in the next section. The adjusted weight loss data were fit with a first-order water release rate, R_L, given by:

$$R_L = -dC/dt = kC \tag{4.4}$$

where C is the concentration of water in the sludge, and $k = k_0 \exp(-Q/T)$ is the first-order rate constant with a pre-exponential factor, k_0 (min^{-1}) and activation energy, Q (K). At constant temperature, k in Equation (4.4) is constant and the equation can be solved to yield:

$$\ln(C/C_0) = -kt \tag{4.5}$$

where C_0 is the concentration at time equals zero. A linear regression fit of the weight loss data was computed using Equation (4.5) to determine the best value for k at 75°C. The adjusted experimental data and the fitted curve for TGA Runs 41 and 45 are shown in Figures 4.2a and 4.2b. The calculated values of k for TGA Runs 40 through 46 are listed in Table 4.2. Comparing the rate constant, k, at 75°C (Table 4.2) with the free water desorption rate constant, k_f (Table 4.1), supports the assumption that the species are different to account for a decrease in the release rate constant with increasing temperature. The lower rate constant (Table 4.2) for the hydrate decomposition at higher temperature compared to the free water desorption rate constant (Table 4.1) is an indication of a stronger bond strength for the hydrated water.

4.2.2 Dehydration Kinetics for the Temperature Range of 75°C to 300°C

A large fraction of the thermal decomposition of hydrated species in K-East canister sludge occurred within the temperature range of 75°C to 300°C. Analysis of the data within this temperature range was performed using a simple mechanistic approach that considered a single-step dehydration of one hydrated species. This was followed by a more realistic approach, given the features of the TGA weight-loss curves, of a multistep decomposition process of one hydrated species. The complicated mechanism involving different hydrated species was not considered in this report, except to mention that some of the impurities affecting the measured data may be ascribed to the other known hydrates of uranium oxides.

4.2.2.1 Single-Step Dehydration Kinetics

The single-step dehydration of a hydrated species of uranium oxide will have the reaction step given in Equation (4.3). Hydrated species that can possibly yield a decomposition reaction in a single step are either $UO_3 \cdot H_2O$ or $UO_4 \cdot 2H_2O$. The single-step reactions for these hydrated species will be

$$UO_3 \cdot H_2O \rightarrow UO_3 + H_2O$$

$$UO_4 \cdot 2H_2O \rightarrow UO_3 + 2H_2O + \tfrac{1}{2}O_2$$

if indeed the experimental data can be represented by a kinetic equation involving one-step decomposition. The implication of a single-step reaction is that the $UO_3 \cdot H_2O$ and $UO_4 \cdot 2H_2O$ were the products of a low-temperature decomposition of the parent hydrates, $UO_3 \cdot 2H_2O$ and $UO_4 \cdot 4H_2O$, respectively.

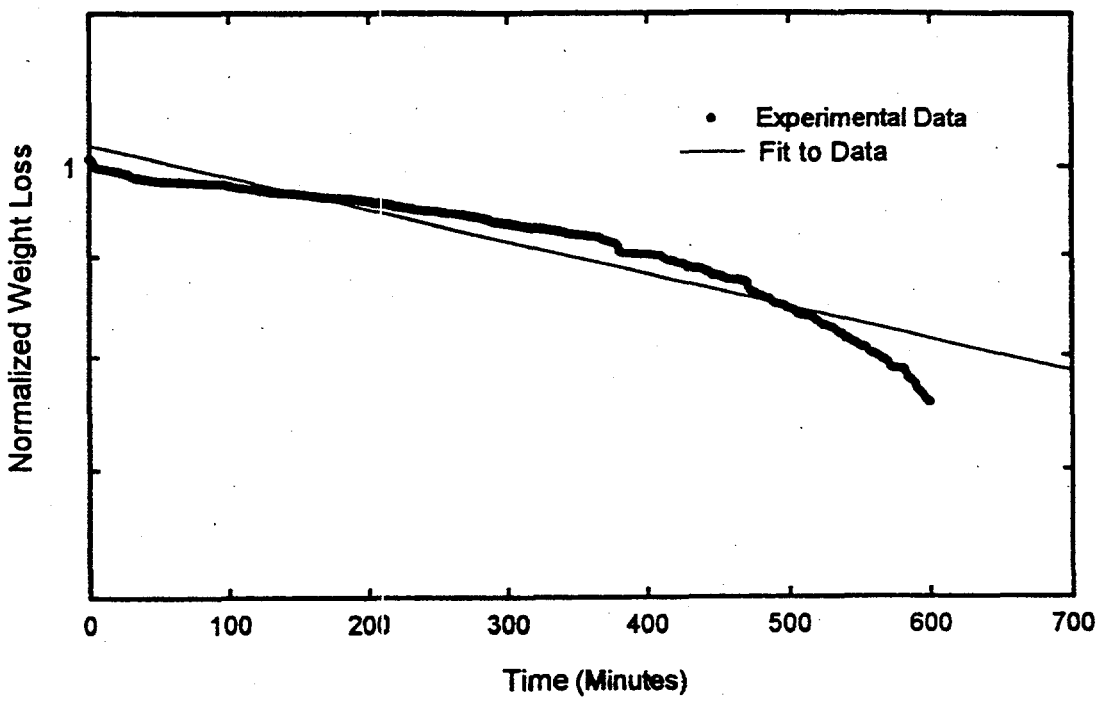

(a)

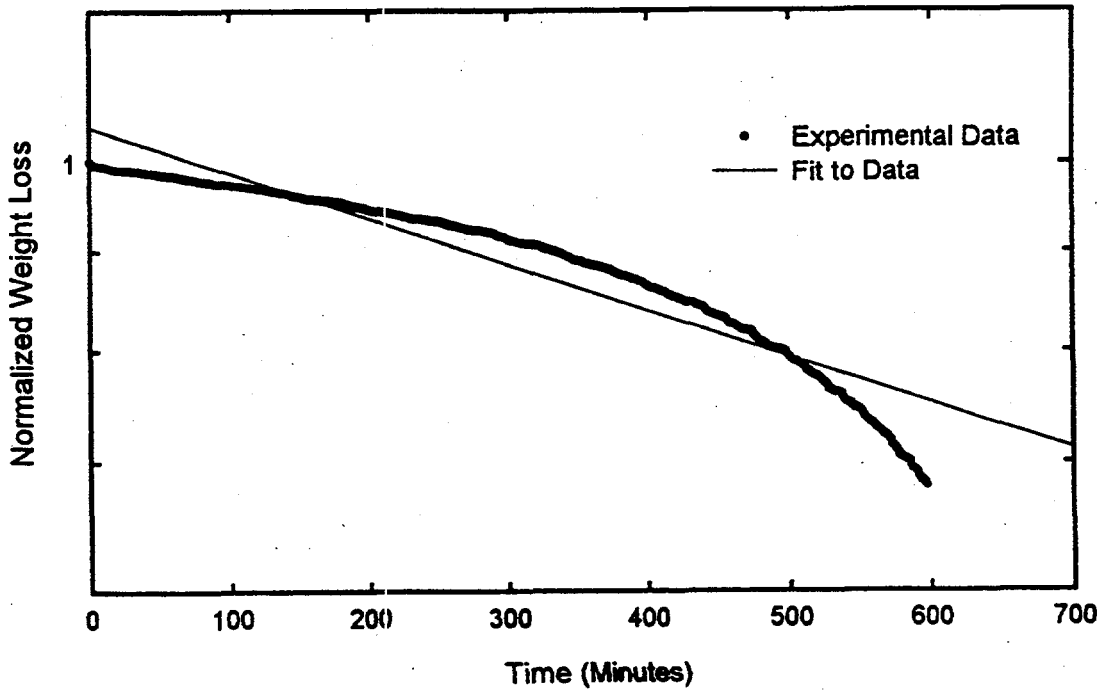

(b)

Figure 4.2. Plots of a Theoretical Fit to the Isothermal Data at 75°C (a) TGA Run 41 and (b) TGA Run 45

Table 4.2. First Peak Decomposition Rate Constant at 75°C

TGA Run	Total First Peak Hydrate (mg)	Weight Loss at 75°C (mg)	Decomposition Rate Constant, k x 10^4 (min^{-1})	r^2 of the fit
40	16.4	3.13	3.27	0.91
41	8.65	2.10	3.83	0.90
42	17.4	6.05	6.52	0.90
43	19.2	0.65	NE	--
44	17.5	2.16	2.13	0.92
45	31.3	9.24	5.47	0.91
46	17.9	9.56	NE	--

NE = Not evaluated (insufficient data for TGA Run 43; hydrate decomposition at 75°C was influenced by free water decomposition for TGA Run 46).

For a single-step kinetics, the dehydration rate is given by Equation (4.4), but the temperature is time dependent, which makes the rate constant, k, also a variable function of time. Solving Equation (4.4) with variable k as function of time yields:

$$\frac{C(t)}{C_0} = \exp\left(-\frac{k_0}{\beta}\theta(T)\right) \tag{4.6}$$

where

$$\theta(T) = \int \exp\left(-\frac{Q}{T'}\right) dT' \tag{4.7}$$

The weight loss data within the temperature range of 75°C to 300°C were normalized with the assumed hydrate content of the sample (i.e., the sum of all the weight losses measured between 75°C and 425°C). The normalized data for TGA Run 45 are plotted (as points) in Figure 4.3. Also shown in Figure 4.3 (as a solid line) is the nonlinear regression fit to the normalized data using Equation (4.6) with two fitting parameters, k_0 and Q. The best-fit curve yielded a rate constant, $k = 24\exp(-4409/T)$ min^{-1}. The shape of the curve does not reproduce the trend in the experimental data curve. This concludes that there is more than one step involved in the decomposition of the hydrated water. The multistep decomposition can be ascribed to multiple reactions from the same starting material or individual decomposition steps from a mixture of different hydrated species. Looking at the weight loss data from TGA Runs 40 through 46, the characteristics of the weight loss data are very similar even though different samples with probably different impurity concentrations were used. This similarity is an indication that

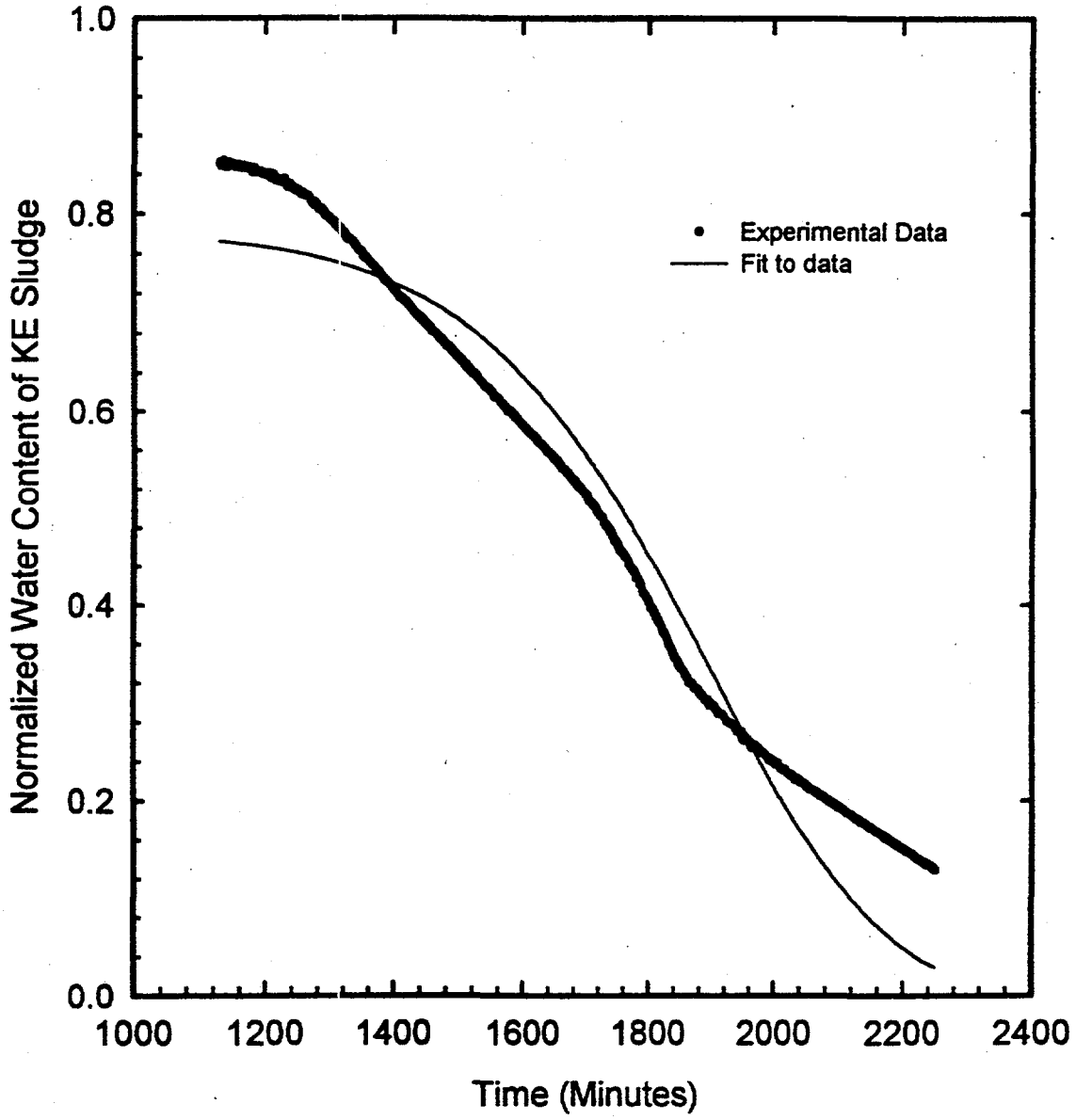

Figure 4.3. Plot Showing the Normalized Weight Loss Data (points) and the Theoretical Fit (solid line) for a Single-Step Dehydration Kinetics

effects of other hydrate impurities on the overall weight loss observed might be small. Hence, the second approach involving a multistep decomposition (which seems to better represent the dehydration data) was analyzed.

4.2.2.2 Multiple Step Dehydration Kinetics

In this section, the weight loss data for the temperature range of 75°C to 300°C (same temperature range fitted with a single species rate constant) were differentiated to give the hydrate decomposition rate as a function of time or temperature. The resulting first derivatives of the weight loss data are plotted in Figures 4.4 through 4.6 and A.8 through A.10. The structure of the decomposition rate curves show three distinct peaks, which suggests a probable decomposition of three different hydrated species, each characterized by a thermal decomposition rate constant. Of the three hydrated species, the other two were considered as products of the previous hydrate.

A uranium oxide hydrate that has been positively identified in K-East canister sludge by XRD (see Figures B.4 and B.6 in Appendix B) is the schoepite phase, $UO_3 \cdot 2H_2O$, which, when comparing the two main forms of uranium oxide hydrates (i.e., trioxide and peroxide hydrates), has been suggested to thermally decompose by three steps. These two factors suggest that the plausible hydrated species present in all the K-East samples was $UO_3 \cdot 2H_2O$. The three probable decomposition steps are shown below:

Decomposition of the dihydrate, $UO_3 \cdot 2H_2O$, to the hydroxide, $UO_2(OH)_2$

$$UO_3 \cdot 2H_2O \rightarrow UO_3 \cdot H_2O + H_2O \tag{4.8}$$

Decomposition of the hydroxide to the hemihydrate, $UO_3 \cdot 0.5H_2O$

$$UO_3 \cdot H_2O \rightarrow UO_3 \cdot 0.5H_2O + 0.5H_2O \tag{4.9}$$

Decomposition of the hemihydrate to uranium trioxide, UO_3

$$UO_3 \cdot 0.5H_2O \rightarrow UO_3 + 0.5H_2O \tag{4.10}$$

However, the observation of a three-step decomposition kinetics of the $UO_3 \cdot 2H_2O$ for the K-East canister sludge may be the first experimental evidence of its kind. Consequently, it could not be ruled out in the decomposition scheme that involves two steps for the $UO_3 \cdot 2H_2O$ phase (for the first and second peaks) and a third peak ascribed to other impurities that could not be identified by the limited sampling for the XRD analysis.

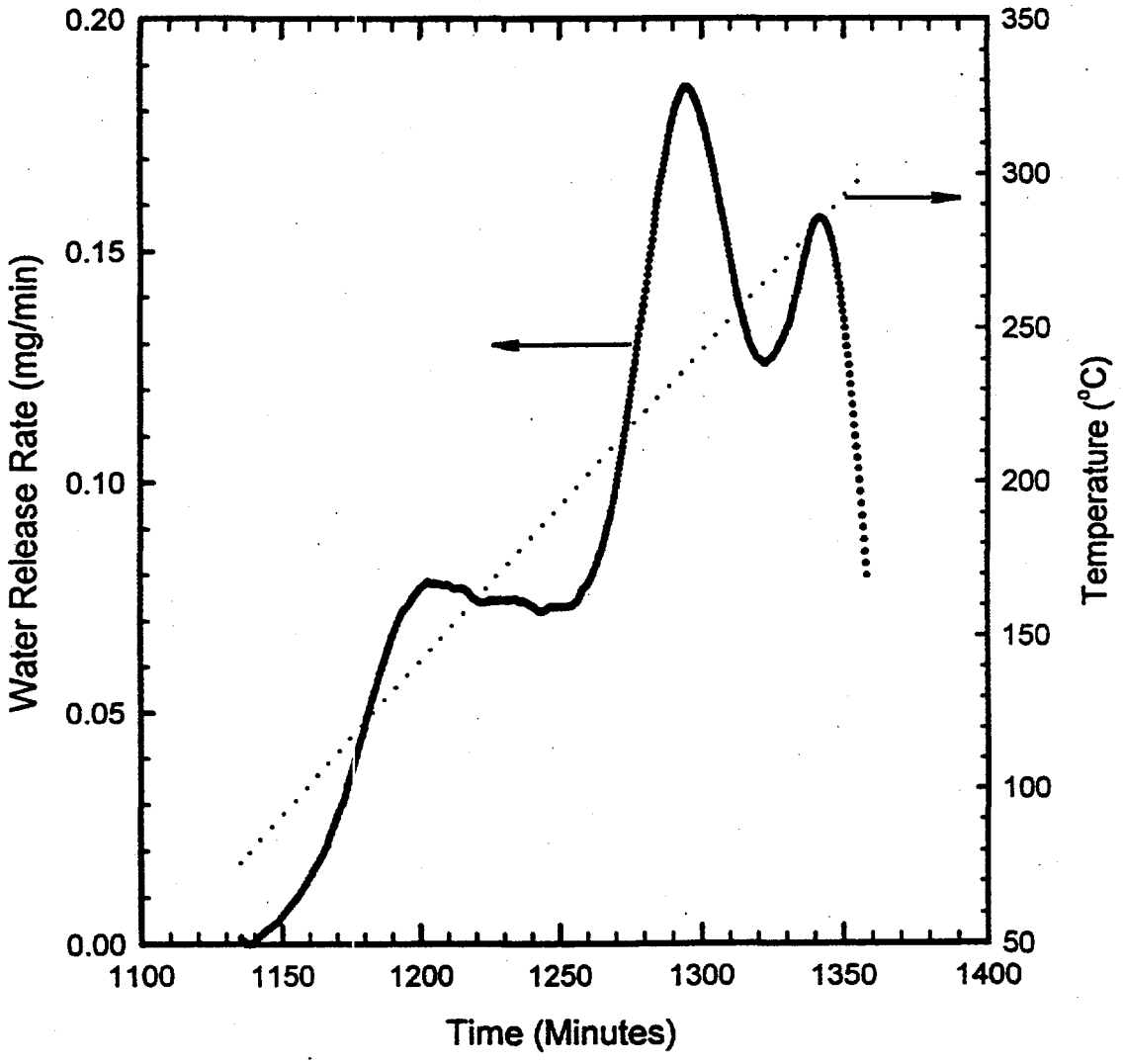

Figure 4.4. Release Rate Curve Showing Three Peaks for TGA Run 40 Data Between 75°C and 300°C

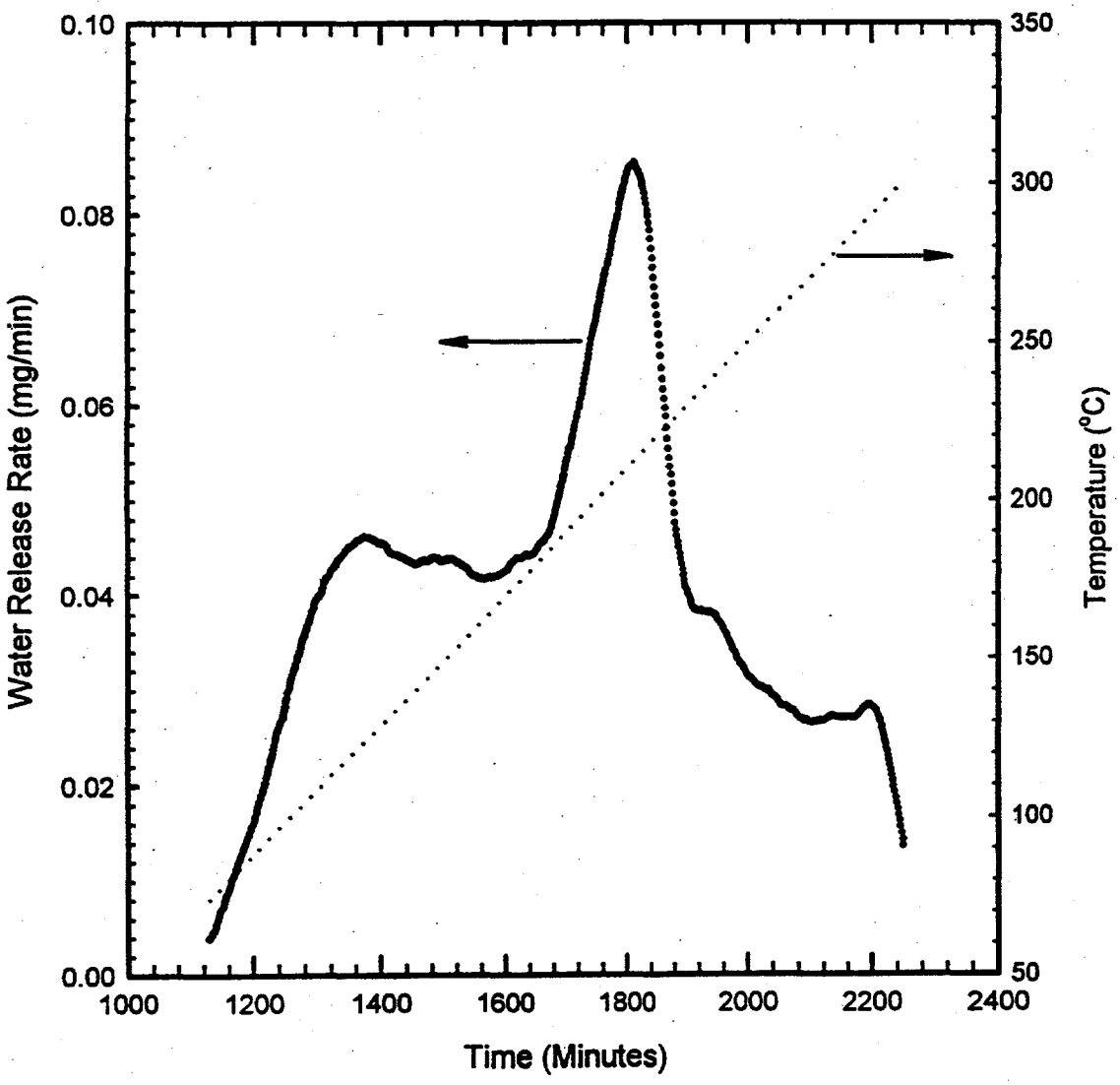

Figure 4.5. Release Rate Curve Showing Three Peaks for TGA Run 45 Data Between 75°C and 300°C

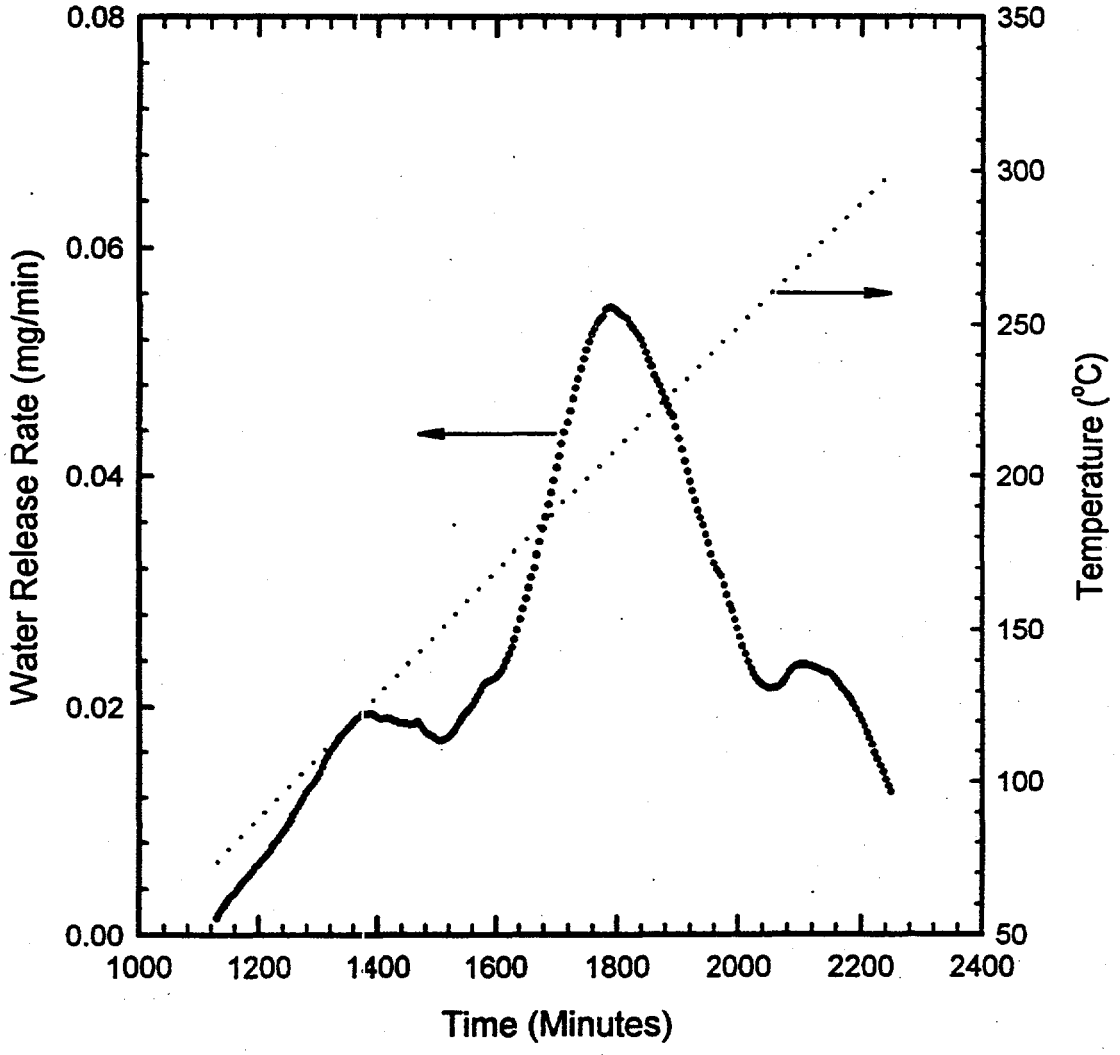

Figure 4.6. Release Rate Curve Showing Three Peaks for TGA Run 46 Data Between 75°C and 300°C

The method of individually determined decomposition rate constant for each peak will be applicable whether the three steps are ascribed to the same or a mixture of hydrated species. The analysis in this section represents the case where all the steps were due to a single hydrated species. The temperature of each peak was graphically determined from the decomposition rate curves (Figures 4.4 through 4.6 and B.5 through B.8), and the results are presented in Table 4.3. Comparisons of the peak temperatures for the two groups (TGA Runs 40 through 42 and TGA Runs 43 through 46) in Table 4.3 clearly show shifts in the peak temperature for all three peaks when the ramp rate was decreased from 1°C/min to 0.2°C/min. For example, the first peak temperature shifted from an average peak temperature of 147°C to 124°C. Theoretically it can be shown that for first-order release kinetics (Abrefah et al. 1991), the shifts in the peak temperature with changes in ramp rate are governed by the equation:

$$\frac{d\ (1/T)}{d\ \ln\ \beta} = -\frac{1}{Q} \tag{4.11}$$

Thus, a plot of 1/T versus lnβ for each peak should be a straight line with a slope of 1/Q. The determined peak temperatures in Table 4.3 are plotted in Figure 4.7. Only two different ramp rate experiments were performed on the K-East canister sludge, and it is inappropriate to determine Q from the plots. However, the general changes in the peak temperatures for the three peaks identified show an indication of first-order thermal decomposition rate kinetics.

Table 4.3. Peak Temperatures for Drying of K-East Canister Sludge

TGA Run	Sample ID	Ramp Rate, β (K/min)	Peak Temperatures (°C)[a]		
			First Peak	Second Peak	Third Peak
40	96-13	1	149	237	284
41	96-13	1	147	223	281
42	96-15	1	144	234	287
43	96-15	0.2	116	212	268
44	96-08	0.2	126	211	274
45	96-04/L	0.2	126	211	270
46	96-08	0.2	128	208	275

(a) Graphically determined from the experimental plots of a water release rate versus time.

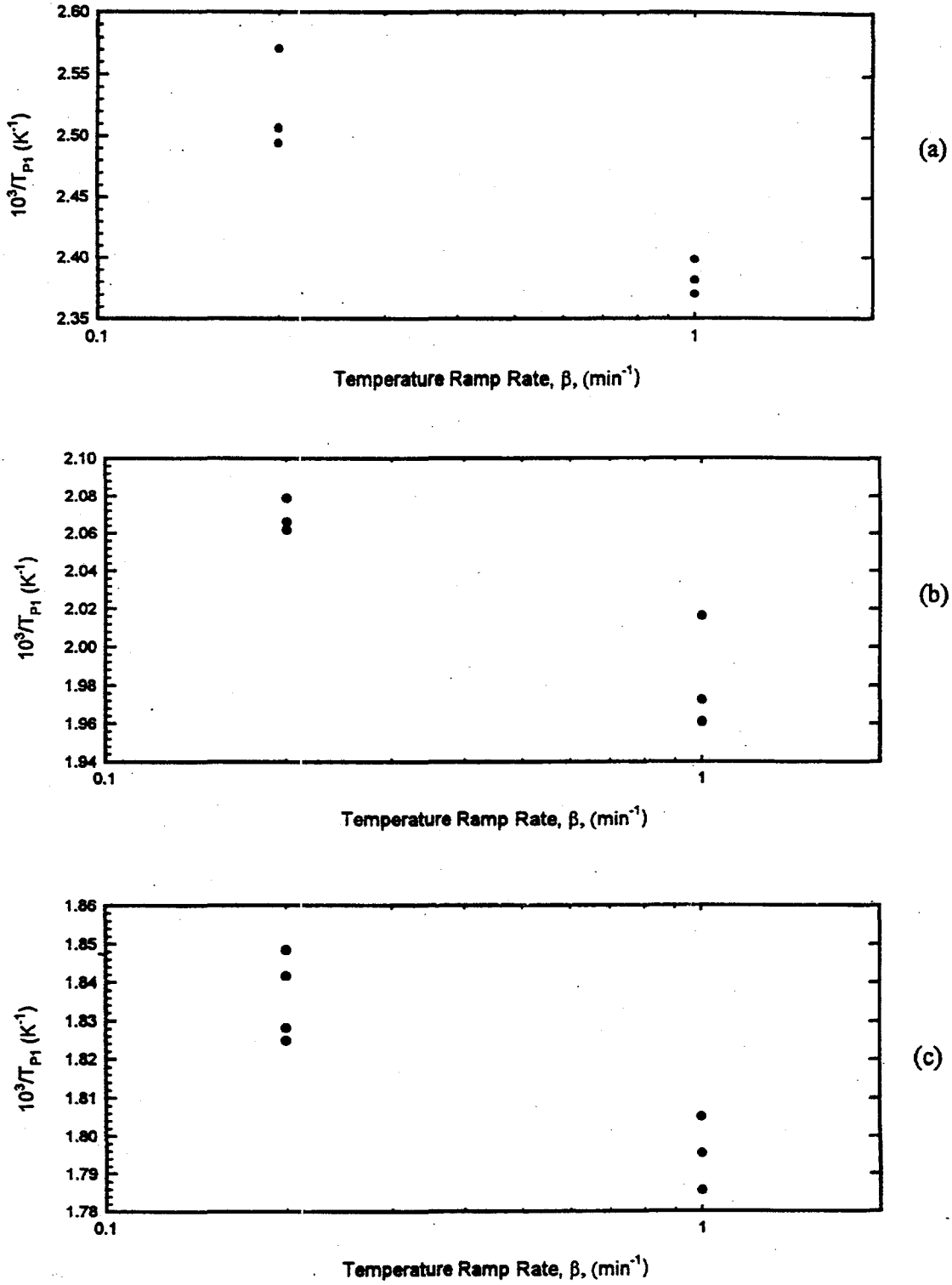

Figure 4.7. Plots of the Peak Temperatures Versus Ramp Rate for the Three Deconvoluted Peaks; (a) First Peak; (b) Second Peak, and (c) Third Peak

The weight loss data within the temperature range of 75°C up to 425°C were broken down into fractions consistent with the mass fractions of Reactions (4.8) through (4.10). Thus, one half of the total weight loss within this temperature range was ascribed to the first peak, and the other half divided equally between the second and third peaks. The result of the breakdown is shown in Table 4.4. As seen in Table 4.4, not all the weight loss conformed to this rigid treatise of the data. There are two instances where the weight loss data could not be used. The first one is for TGA Run 40, where the sum of weight loss at 300°C and between 300°C and 425°C is greater than the estimated amount for the third peak. This may have been caused by impurities in the sample that may have decomposed within this temperature range, accounting for the additional weight loss, or purely due to experimental variability. The second discrepancy is the weight loss at 75°C for TGA Run 46. However, this is more likely due to the influence of free water that was not completely removed by drying at temperatures below 75°C.

The dehydration rate constant for each of the three peaks was determined by a method analogous to thermal desorption kinetics from surfaces (Dawson and Walker 1976 and Tanabe et al. 1987). The analysis of the peaks of the decomposition rate curves involved deconvolution of the peaks by a graphical method. The separated individual peaks were checked theoretically with a release kinetics that is diffusion rate limited. A complete discussion of the diffusion control analysis is given in Abrefah et al. (1991). Also, from the discussion of the shift in the peak temperature (in the preceding paragraph), only first-order kinetics will be fitted to the deconvoluted peaks. The decomposition rate kinetics from Equations (4.4) and (4.6) is given as:

$$R_L = k_0 C_0 \exp\left\{ -\frac{k_0}{\beta}\Theta(T) - Q/T \right\} \tag{4.12}$$

where $\Theta(T)$ is given by Equation (4.7), β is the temperature ramp rate, C_0 is the initial concentration of species analyzed (i.e., the integral under each peak). At the maximum release rate Equation (4.12) can be solved to yield:

$$k_o = \left(\beta Q/T_p^2\right)\exp\left(Q/T_p\right) \tag{4.13}$$

A nonlinear regression fit of the first peak data was computed using Equation (4.12) with the constraint that the rate constant, k, at 75°C is equal to what was determined for the isothermal release and listed in Table 4.2. In the cases where k at 75°C was not determined, values obtained from other runs for the same sludge sample were used. Thus, for TGA Run 43, k for TGA Run 42 was used and for TGA Run 46, k for TGA Run 44 was used. The second and third peaks were fitted with the constraint that the pre-exponential factor, k_0, is given by Equation (4.13) to determine k_0 and Q. The pre-exponential factors and the activation energies for the last seven K-East canister sludge tests are listed in Table 4.5. There is good agreement between the activation energies for all the runs, but there is a large spread of data among the pre-exponential factors. The reason for the spread in the pre-exponential is not very obvious from the analysis, but it could have been influenced by not starting with a pure hydrated sample (i.e., free water effect).

Table 4.4. Deconvoluted Hydrated Species of K-East Canister Sludge

TGA Run	Total 75 to ≤ 425°C	Peak 1 (mg)			Peak 2, 75 to 300°C (mg)	Peak 3 (mg)			
		Total	At 75°C	75 to 300°C		Total	75 to 300°C	At 300°C	300 to 425°C
40	32.76	16.38	3.13	13.25	8.19	8.19	NE[a]	7.25	1.55
41	17.29	8.65	2.10	6.55	4.32	4.32	0.93	2.75	0.64
42	34.72	17.36	6.05	11.31	8.7	8.66	2.17	4.56	1.93
43	38.41	19.21	0.65	18.56	9.6	9.6	5.23	3.84	0.53
44	35.01	17.51	2.16	15.35	8.75	8.75	3.92	2.52	2.31
45	62.67	31.34	9.24	22.10	15.7	15.63	6.90	4.10	4.63
46	35.87	17.94	9.56[b]	15.74	9.0	8.93	3.57	3.18	2.18

(a) The sum of weight losses at 300°C and between 300°C up to 425°C is greater than what is estimated to be the weight loss for the third peak.

(b) The weight loss at this temperature was strongly influenced by the free water desorption and was not used in the analysis of hydrate decomposition. Instead, the weight loss value for Run 44 at 75°C was used.

Table 4.5. Decomposition Parameters of K-East Canister Sludge

TGA Run	Pre-exponential Factors, k_0 (min^{-1})			Activation Energies, Q (K)		
	Peak 1	Peak 2	Peak 3	Peak 1	Peak 2	Peak 3
40	2253	56000	15600	5504	7308	7540
41	16000	19900	11500	6010	6750	7350
42	40000	59400	10100	6104	7300	7515
43	24	48100	6700	3687	7550	7700
44	324	28000	4400	5000	7200	7500
45	238	11000	1400	4471	6950	7480
46	326	56700	4513	5003	7630	7754

The individual release curves resulting from the theoretical fit to the experimental data are shown together with the data in Figure 4.8. The figure shows a good representation of the experimental data by the multistep reactions. Each reaction step gives a corresponding release rate curve. The sum of the three individual release curves is plotted in Figure 4.9 and compares reasonably well with the experimental release curves.

4.3 Oxygen Evolution from Dehydrated Sludge

The $UO_3 \cdot 2H_2O$ phase was assumed for the mechanistic analyses of the K-East canister sludge weight loss data. Consequently, the limited hydrated water content of the sludge is theoretically estimated to be 11.2 wt% in the sludge. In TGA Run 45, the total weight loss by the sample, excluding all the free water components, was 68.34 mg. This weight loss translates to 14.5 wt% based on the initial sample weight and 16.0 wt% based on the dried sample weight (i.e., initial sample weight minus all the free water weight). There are two probable explanations for this difference in weight fraction of the sludge compared to the theoretical weight fraction:

1. Weight loss at higher temperatures ($\geq$ 425°C) was due to reduction of uranium oxide.

2. Impurities in the sludge could be the hydrates of uranium peroxide and/or iron oxide and alumina.

Oxygen evolution by a reduction reaction of the dried uranium oxides was assumed to be the major effect in causing the sample weight loss at higher temperatures, because the impurities mentioned were not identified in the limited XRD examinations performed. Additionally, the reduction reaction of UO_3 to U_3O_8 at these temperatures is consistent with observations of others (Wheeler et al. 1964 and Hoekstra and Siegel 1973), who have studied dehydration of the $UO_3 \cdot 2H_2O$ phase. The reduction reaction of

$$3UO_3 \rightarrow U_3O_8 + \tfrac{1}{2}O_2$$

gives additional theoretical weight loss of about 2 wt%. Thus, a total theoretical weight loss of about 13.2 wt% is expected for a pure $UO_3 \cdot 2H_2O$ sample if the end product is U_3O_8. Based on the dried sludge sample weight (i.e., excluding all free water), the oxygen evolution measured for the last seven sludge samples ranges from 0.2 wt% to 1.3 wt%. This excludes the data from the tests in which two samples were reheated to 1000°C (TGA Runs 42 and 45), which also showed evidence of further reduction reactions that resulted in additional sample weight loss.

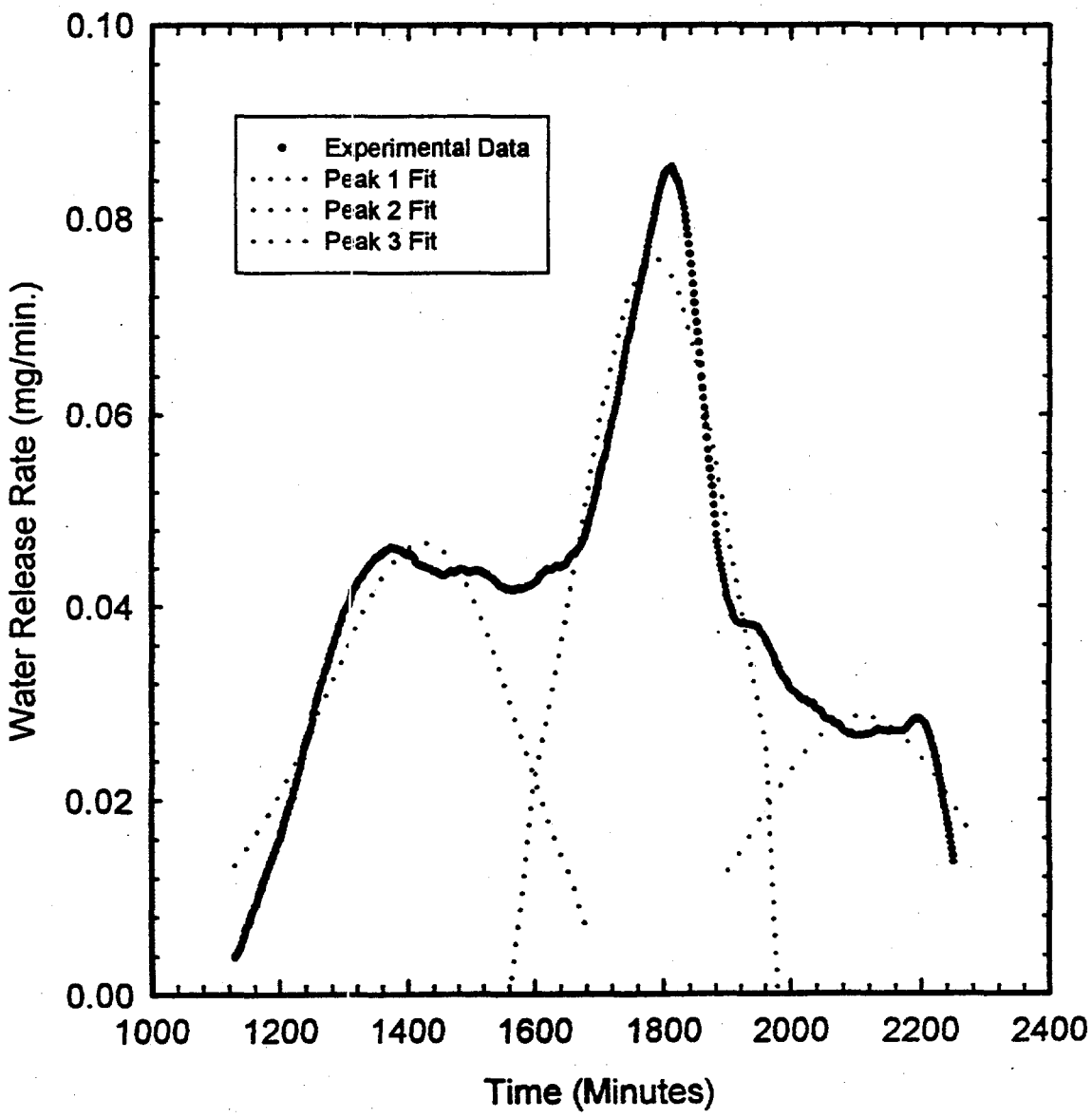

Figure 4.8. The Three Theoretical Release Peaks and the Experimental Release Data for TGA Run 45

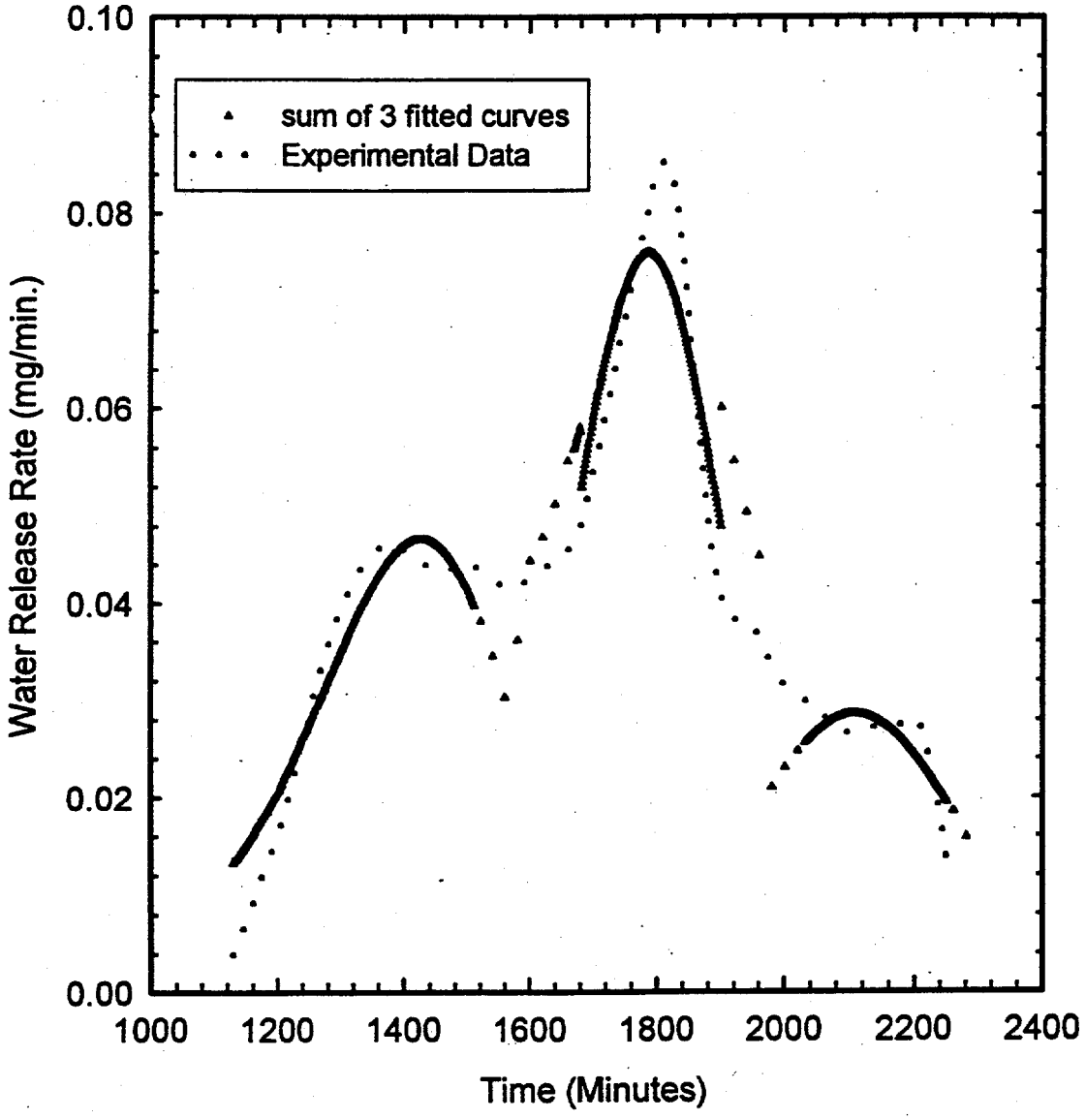

Figure 4.9. Plot of the Sum of the Three Theoretical Release Peaks and the Experimental Release Rate Data for TGA Run 45

5.0 Discussion

Calculated sample weight losses for seven sludge drying tests are listed in Table 3.2. By attributing the weight loss to thermal decomposition of the hydrated species, the bound water content in the sludge samples ranges from 3 wt% to 15 wt% (based on the initial sample weight). X-ray diffraction analyses of K-East canister sludge samples have confirmed the presence of a trioxide hydrate phase, $UO_3 \cdot 2H_2O$. The characteristic three-step reaction shown by the thermal decomposition data also supports the presence of the $UO_3 \cdot 2H_2O$ form of hydrate. Based on these observations, it can be assumed that the K-East canister sludge contains the $UO_3 \cdot 2H_2O$ phase, and thus the theoretical maximum weight fraction of the water in the hydrated portion of the sludge would be 11.2 wt%. The maximum weight fraction observed in TGA Run 45 (Table 3.2) is greater than this theoretical estimate. The possible reasons for the additional weight loss are shown below:

1. possible impurity contribution by other hydrates and hydroxides of the uranium and/or iron oxide such as the peroxide (i.e., $UO_4 \cdot xH_2O$; $2<x<4$) and $UO_2(OH)_2$

2. contributions from oxygen evolution at higher temperatures by reduction reaction of the higher oxides of uranium (e.g., $3UO_3 = U_3O_8 + \frac{1}{2}O_2$)

3. residual free water contribution to the total weight loss, especially below 75°C.

Since the $UO_4 \cdot xH_2O$ phase has not been identified by the XRD analysis, its effect may be insignificant. Thus, the other factors (2 and 3) may be the main reason for the increased weight loss above the expected theoretical estimate for TGA Run 45. The observation of a low-temperature effect of free water on the total weight loss and the oxygen decomposition at higher temperatures might be applicable to all the runs and, therefore, was considered in analyzing the weight loss data for hydrate decomposition kinetics.

Excluding the free water component in TGA Run 46, the largest fraction of the hydrate(s) thermally decomposed within the temperature range of 75°C to 300°C for all the tests. Slowing the heating rate (0.2°C/min) caused most of the hydrated species present to decompose during the (approximately) 19-hour period it took to reach 300°C. The temperature response of the first 10 runs for this temperature range with a faster ramp rate (1°C/min) showed a faster release of the moisture from the sample.

In TGA Run 46, a fraction of the physically bound water was still present after the first temperature drying segment of ambient to 50°C. Evidence of this remaining fraction was found by comparing the weight loss during the second temperature segment for TGA Runs 44 and 46 (the two runs used a test subsample taken from the same K-East canister sample, 96-08). The weight loss in TGA Run 46, which started with a large fraction of free water left in the sample due to changes in the experimental steps and conditions (1-hour pumpdown for Run 46 versus 24 hours pumpdown for Run 44), is about five times greater than the weight loss in TGA Run 44. Thus, a flowing gas environment at 50°C for 10 hours was not adequate to dry/remove all the free water in the sludge. This observation supports the inference that

in all the runs, a small fraction of the physically bound water can remain in the sample after the initial ambient temperature pumpdown, which appears to be released during the first heating segments of the tests. The leftover physically bound water may have contributed to the increased weight loss (above the theoretical expectation) for the sludge sample in TGA Run 45.

The free water content of the sludge samples tested ranges from as low as 7 wt% to 64 wt%. This calculation was based on the assumption that all the free water content of the sludge was released during the system pumpdown period plus a small fraction between ambient temperature up to 75°C. The amount of free water content measured indicates a high water content sludge sample. This suggests the K-East canister sludge consists of very finely divided particulates or materials that are porous, giving a very high surface area for adsorption and absorption of water molecules.

The thermal decomposition kinetics of the hydrates for the test conducted in the flowing ultra high purity helium (TGA Run 46) compared to the vacuum test (TGA Run 44) did not show a significant difference in release rate. The significant fraction of free water released for TGA Run 46 after the ambient temperature up to 75°C segments of heating indicates a possible slowdown in the release of free water in a flowing gas medium.

The breakdown of the overall weight loss data into three regions with discrete boundaries during the mechanistic analysis of the data did not yield a perfect match. However, it provided reasonable separation of the weight loss data into three regions. The three regions were then attributed to reactions that involved desorption of physically bound water, dehydration of chemically bound water, and reduction of uranium oxide(s).

The supporting data for the desorption of free water at temperatures below 75°C are the rate constants listed in Table 4.1 for the isothermal data at 50°C and Table 4.2 for 75°C. The averaged rate constants for desorption in the two tables are 4.8×10^{-3} min^{-1} for 50°C and 4.2×10^{-4} min^{-1} for 75°C. The only probable explanation for the lower rate at 75°C is desorption from a different chemical species. The deviation of the drying mechanism from the assigned rigid boundaries for the analysis may affect the end results of the determined parameters. The free water desorption will affect the dehydration kinetics of the first peak. The analysis of the third peak could have been affected by oxygen evolution from the sludge. The significance of these effects on the determined rate constants could not be ascertained from the experimental data.

6.0 Conclusions

All the K-East canister sludge samples lost weight within the temperature range of ambient to 1000°C. The weight loss was due to release of physically bound water and chemically bound water, and oxygen evolution by the reduction of uranium oxide(s).

Large fractions of the physically bound water were released at ambient temperature during the initial system pumpdown to the desired test vacuum conditions over a 24-hour period. The physically bound water fractions of the samples range from 7 wt% and 64 wt%, suggesting K-East canister sludge is a highly porous medium with a large surface area for adsorption and absorption of water.

The free water in the sludge was not completely removed after a period of 10 hours at 50°C in an atmosphere of ultra high purity helium. Consequently, the sludge samples that had free water remaining prior to heating released their residual free water between the temperature range of ambient to 75°C. However, the free water drying for the samples tested in vacuum was more effective than the test performed in atmospheric helium, suggesting that

- Free water release kinetics may be enhanced by reduced pressure (vacuum conditions), and
- Drying of free water in helium at atmospheric pressure takes more than 10 hours.

The mechanistic analysis indicates that the thermal decomposition of the hydrated species effectively starts at temperatures about 75°C. The dehydration rate was ramp rate dependent. The decomposition rate of the hydrate in vacuum and ultra high purity helium environment at atmospheric pressure showed no significant differences.

The release rate curve for the last seven TGA runs indicates the thermal decomposition of the hydrated species occurred as a three-step reaction. The three-step reactions can be explained if the starting material is assumed to be uranium trioxide hydrate, which gives the following decomposition reactions:

1. Decomposition of the dihydrate, $UO_3 \cdot 2H_2O$, to the hydroxide, $UO_2(OH)_2$

$$UO_3 \cdot 2H_2O \rightarrow UO_3 \cdot H_2O + H_2O$$

2. Decomposition of the hydroxide to the hemihydrate, $UO_3 \cdot 0.5H_2O$

$$UO_3 \cdot H_2O \rightarrow UO_3 \cdot 0.5H_2O + 0.5H_2O$$

3. Decomposition of the hemihydrate to uranium trioxide, UO_3

$$UO_3 \cdot 0.5H_2O \rightarrow UO_3 + 0.5H_2O$$

The positive identification of the schoepite phase in the canister sample 96-04/Lower by XRD supports the conclusion that the hydrated species may be a uranium trioxide hydrate, $UO_3 \cdot 2H_2O$.

The temperature at which the hydrate decomposition rate is at its maximum (i.e., peak temperature) was determined for each decomposition step. The averaged peak temperatures for the two ramp rates of 1°C/min and 0.2°C/min are as follows:

- first peak; 147°C and 124°C
- second peak; 231°C and 211°C
- third peak; 284°C and 272°C.

The three peak temperatures shifted with changes in the ramp rate. Decreasing the heatup rate decreased the peak temperature. These peak temperatures suggest heat treatment temperatures necessary for drying the corresponding hydrated species.

The activation energies obtained by the analysis of the experimental data using first-order kinetics are within expectation. However, the pre-exponential factors are relatively low for first-order kinetics and showed more spread. The close agreement of the activation energies suggests that the peak temperatures predicted by the three-step decomposition mechanism represent the optimal temperatures for heat treatment of the hydrated species present in the K-East Basin canister sludge. The large spread of the pre-exponential factors may be due to simplification in the deconvolution of the weight loss data into individual components of the three reaction steps. Additional experiments involving a continuous temperature ramp and sampling of the sludge in-between runs will be necessary to accurately determine the pre-exponential factors.

From the results of the drying tests on K-East canister sludge, it can be concluded that a heat treatment process similar to the steps used in this study is adequate to thermally decompose most of the hydrated species.

7.0 References

Abrefah, J., D. R. Olander, and M. Balooch. 1991. "Hydrogen Dissolution In and Release From Nonmetals. II. Crystalline Silicon." *J. Applied Physics* 67(7):3302.

Abrefah, J., W. J. Gray, G. L. Ketner, S. C. Marschman, T. D. Pyecha, and T. A. Thornton. 1996. *K-Basin Spent Nuclear Fuel Characterization Data Report II.* PNNL-10944, Pacific Northwest National Laboratory, Richland, Washington.

Boggs, J. E., and M. El-Chehabi. 1957. "The Thermal Decomposition of Uranium Peroxide, $UO_4 \cdot 2H_2O$." *J. American Chemical Society* 79:4258.

Cordfunke, E.H.P. 1961. "Alpha-UO_3: Its Preparation and Thermal Stability." *J. Inorg. Nucl. Chemistry* 23:285.

Cordfunke, E.H.P, and A. A van der Giessen. 1963. "Pseudomorphic Decomposition of Uranium Peroxide Into UO_3." *J. Inorg. Nucl. Chemistry* 25:553.

Dawson, P. T., and P. C. Walker. 1976. "Experimental Methods in Catalytic Research," Eds., R.B. Anderson and P.T. Dawson, Vol. III, p. 211. Academic, New York.

Hoekstra, H. R., and S. Siegel. 1973. "The Uranium Trioxide-Water System." *J. Inorg. Nucl. Chemistry* 35:761.

Katz, J. J., and E. Rabinowitch. 1951. "The Chemistry of Uranium: The Element, Its Binary and Related Compounds." National Nuclear Energy Series, Manhattan Project Technical Section, Division VIII - Volume 5, Dover Publications, New York.

Makenas B. J., et al. 1996. *Analysis of Sludge from Hanford K East Basin Floor and Weasel Pit.* WHC-SP-1182, Westinghouse Hanford Company, Richland, Washington.

Makenas B. J., et al. 1997. *Analysis of Sludge from Hanford K East Basin Canisters.* HNF-SP-1201, Duke Engineering & Services Hanford, Inc., Richland, Washington.

Poko, Z., M. Fodor, and E. Szabo. 1968. *Acta Chim. Acad. Sc. Hung* 56:357.

Sato, T. 1963. "Preparation of Uranium Peroxide Hydrates." *Journal of Applied Chemistry* 13:361.

Tanabe, T., H. Hirano, and S. Imoto. 1987. *J. Nuclear Materials* 151:38.

Taylor, P., D. D. Wood, A. M. Duclos, and D. G. Owen. 1989. "Formation of Uranium Trioxide Hydrates on UO_2 Fuel in Air-Steam Mixtures Near 200°C." *Journal of Nuclear Materials* 168:70.

Westinghouse Hanford Company (WHC). 1995. *Hanford Spent Nuclear Fuel Project Integrated Process Strategy for K Basins Spent Nuclear Fuel.* WHC-SD-SNF-SP-005, Rev. 0, July 1995, Richland, Washington.

Wheeler, V. J., R. M. Dell, and E. Wait. 1964. "Uranium Trioxide and the UO_3 Hydrates." *J. Inorg. Nucl. Chemistry* 26:1829.

Appendix A

K-East Canister Sludge Drying Results

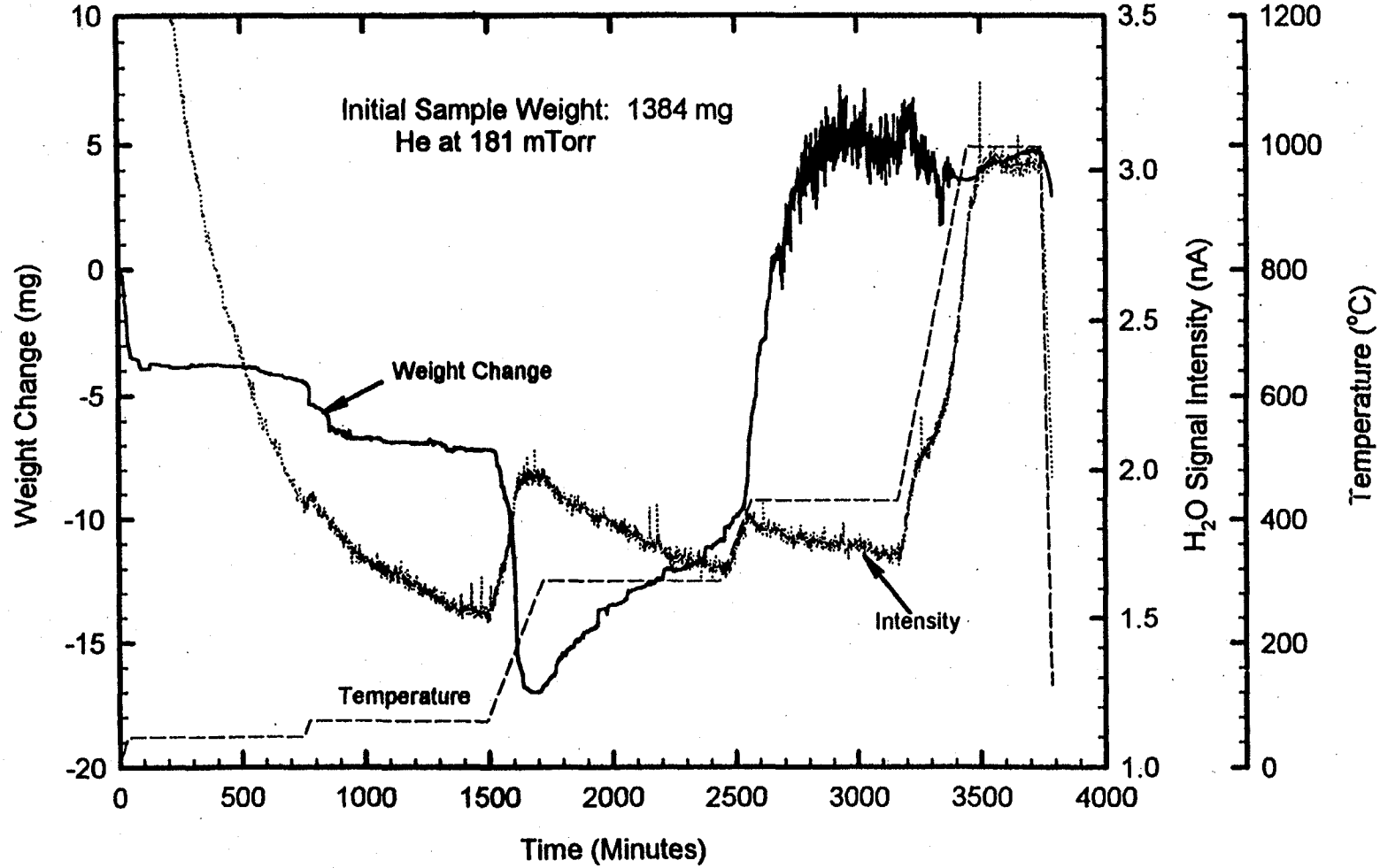

Figure A.1. TGA Run 31 Plot Showing Weight Change, MS Signal for H_2O, and Temperature Versus Time for KE Canister Sludge 96-05

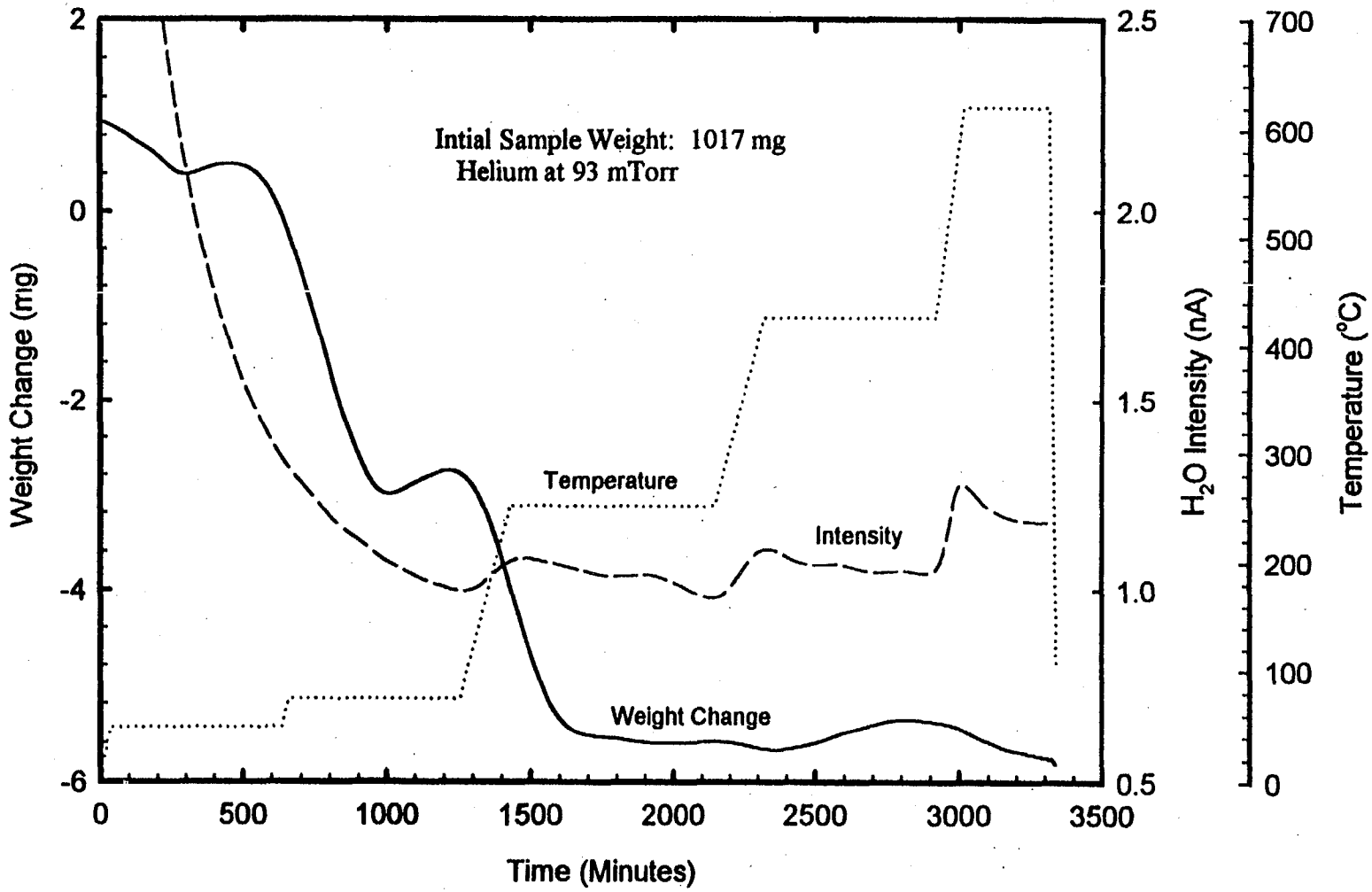

Figure A.2. TGA Run 32 Plot Showing Weight Change, MS Signal for H_2O, and Temperature Versus Time for KE Canister Sludge 96-05

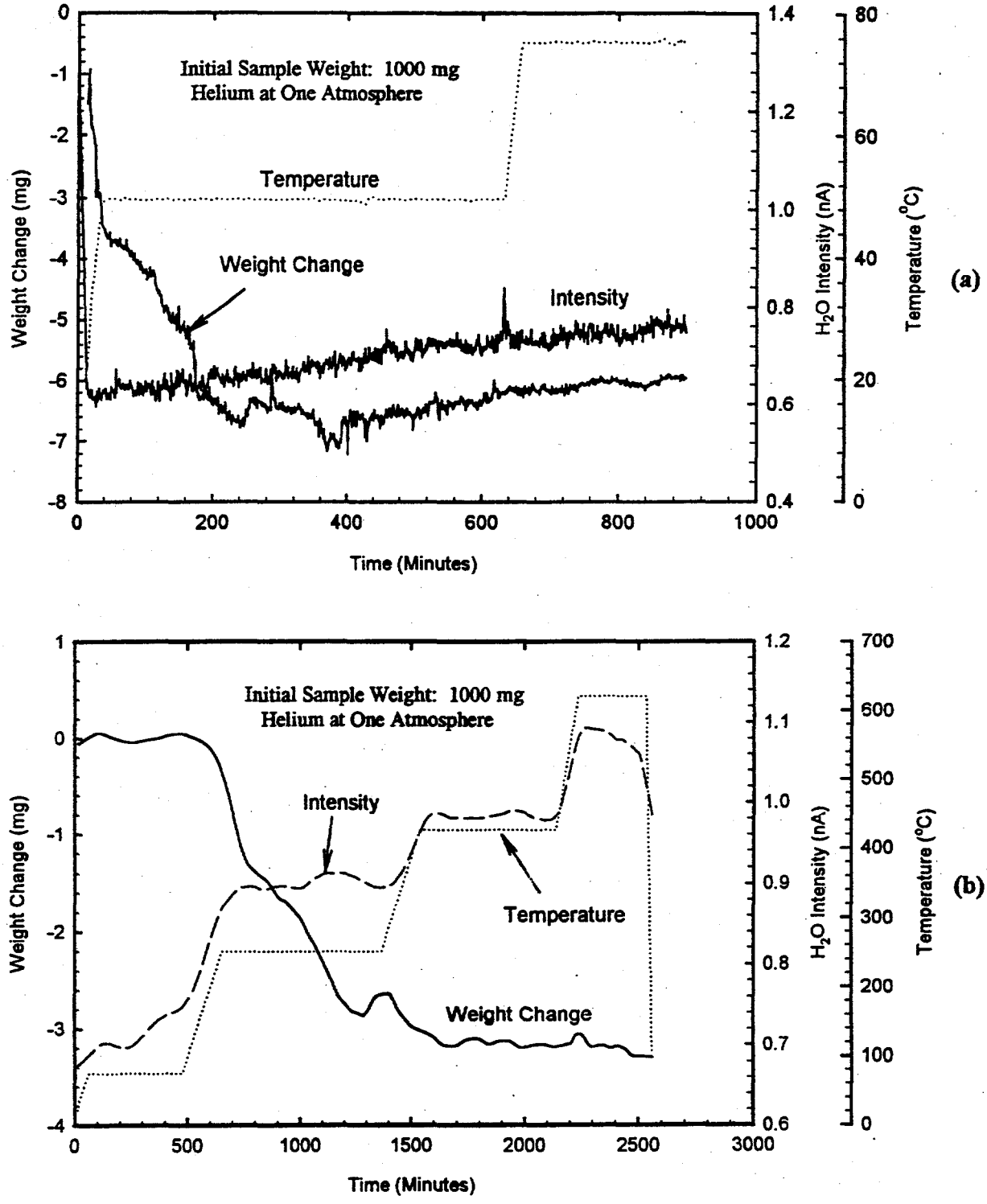

Figure A.3. TGA Run 33 Plots Showing Weight Change, MS Signal for H_2O, and Temperature Versus Time: (a) First Two Segments and (b) Remaining Segments for KE Canister Sludge 96-05

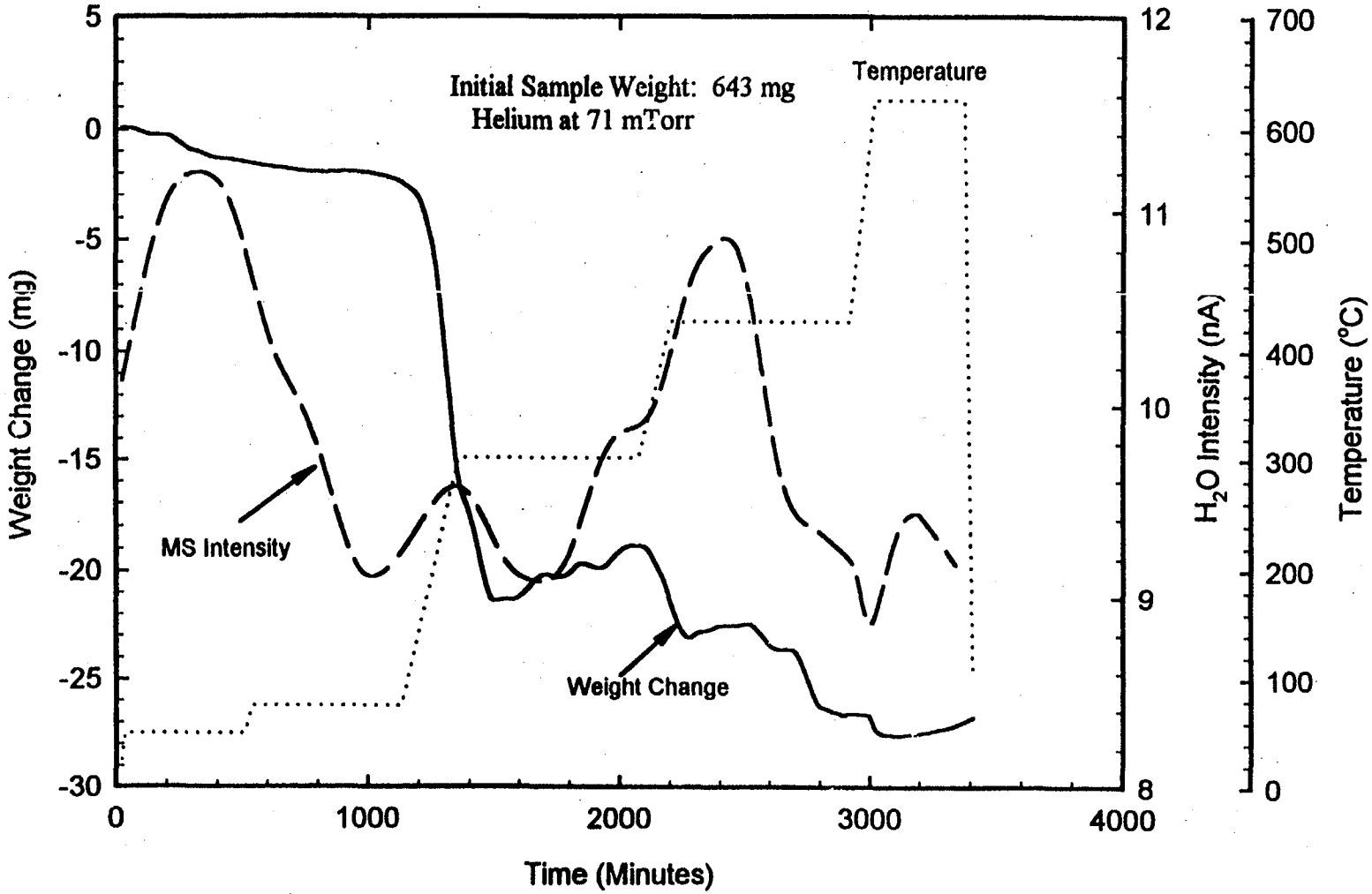

Figure A.4. TGA Run 36 Plot Showing Weight Change, MS Signal for H_2O, and Temperature Versus Time for KE Canister Sludge 96-01

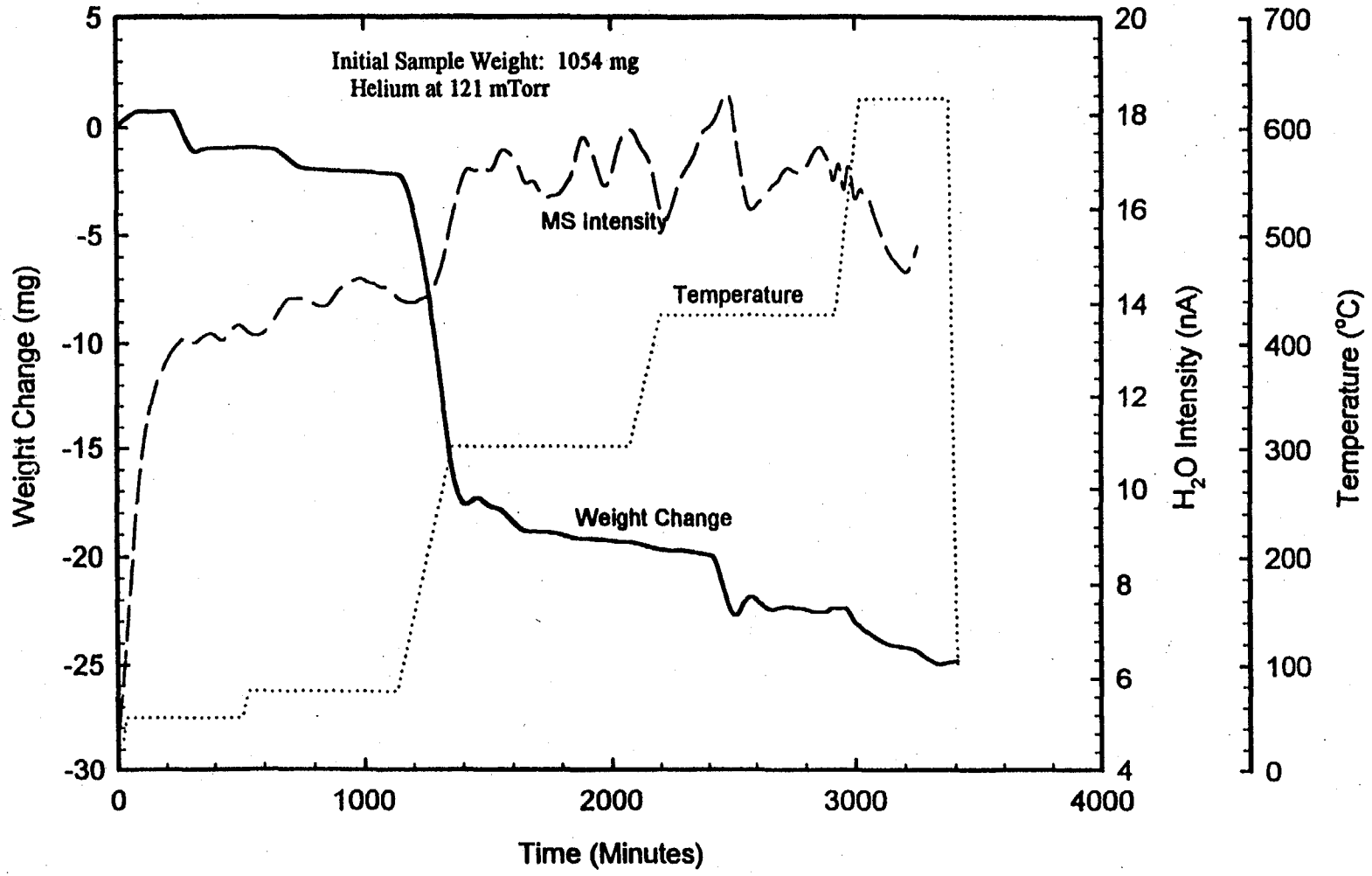

Figure A.5. TGA Run 37 Plot Showing Weight Change, MS Signal for H_2O, and Temperature Versus Time for KE Canister Sludge 96-01

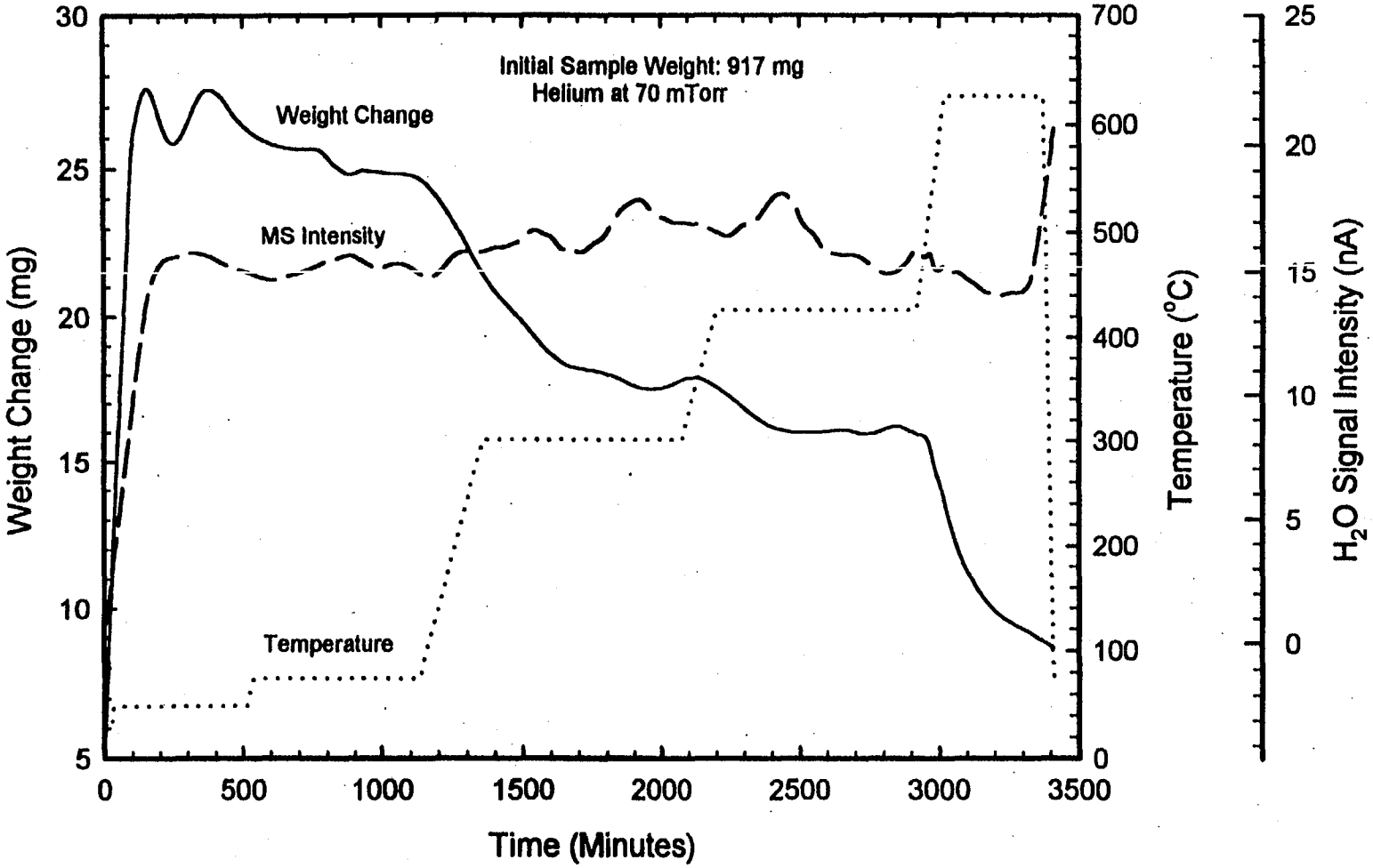

Figure A.6. TGA Run 38 Plot Showing Weight Change, MS Signal for H_2O, and Temperature Versus Time for KE Canister Sludge 96-08

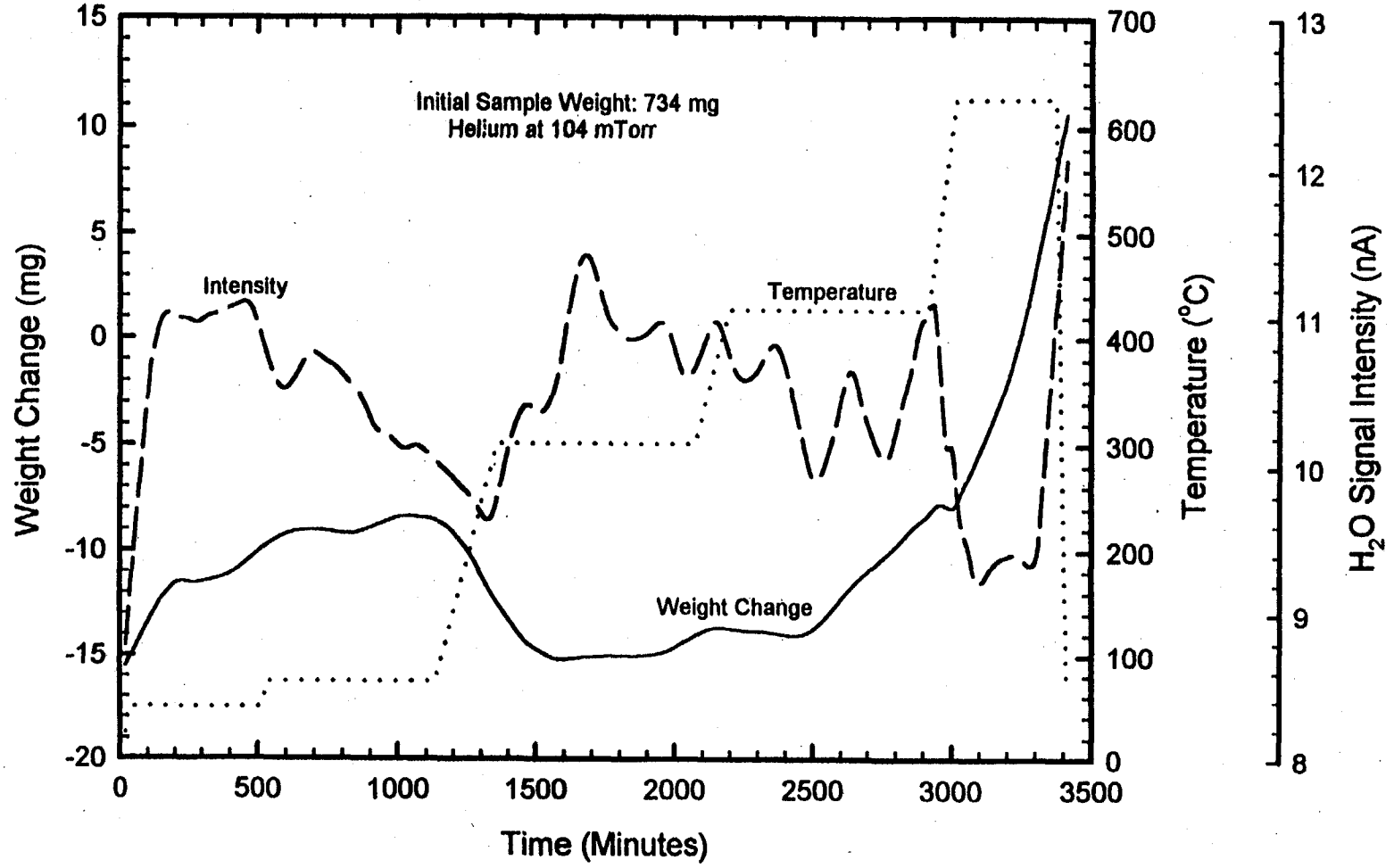

Figure A.7. TGA Run 39 Plot Showing Weight Change, MS Signal for H_2O, and Temperature Versus Time for KE Canister Sludge 96-08

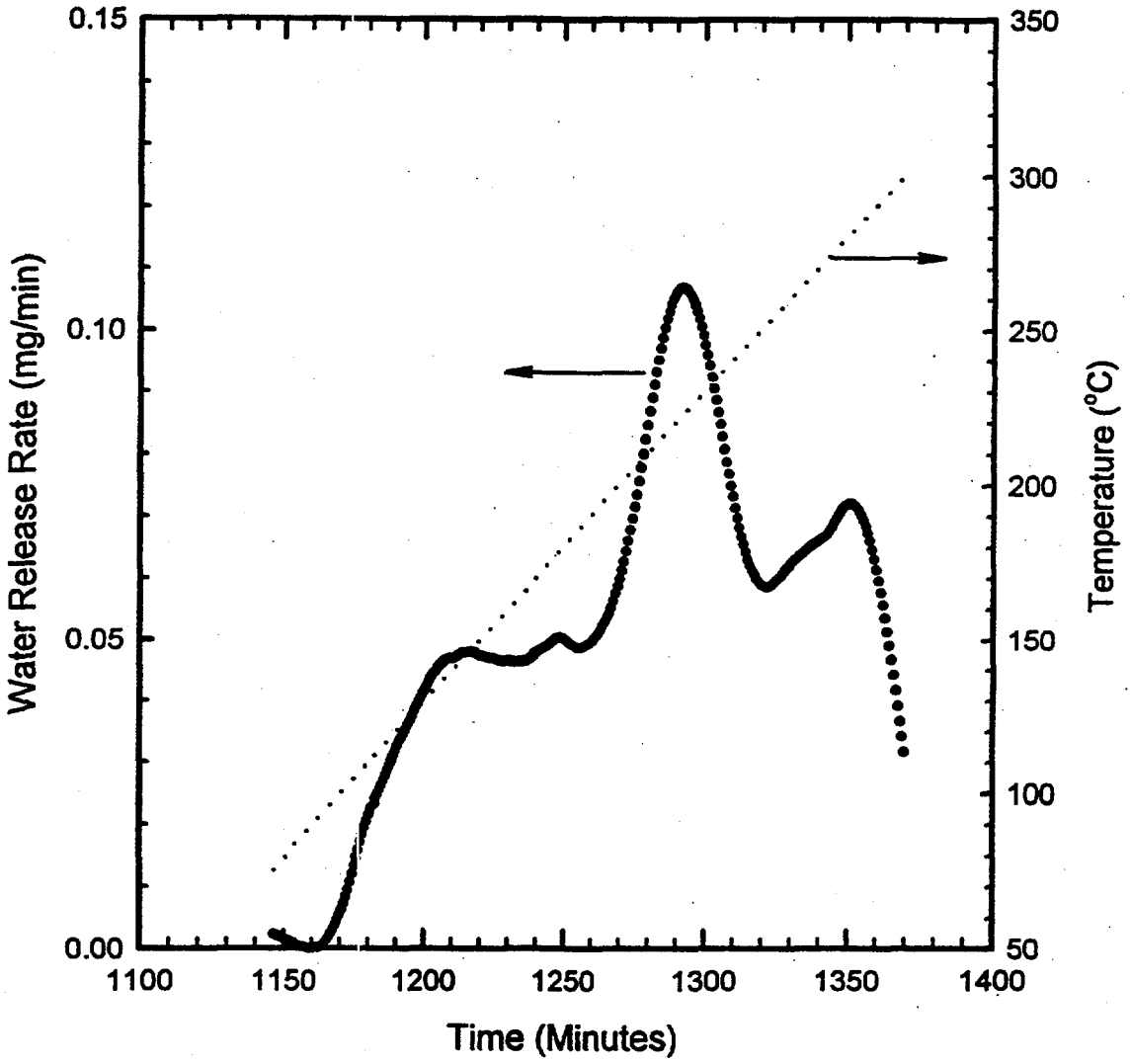

Figure A.8. Release Rate Curve for the Transient Temperature Data Between 75°C and 300°C for TGA Run 41, Indicating Three Different Peaks

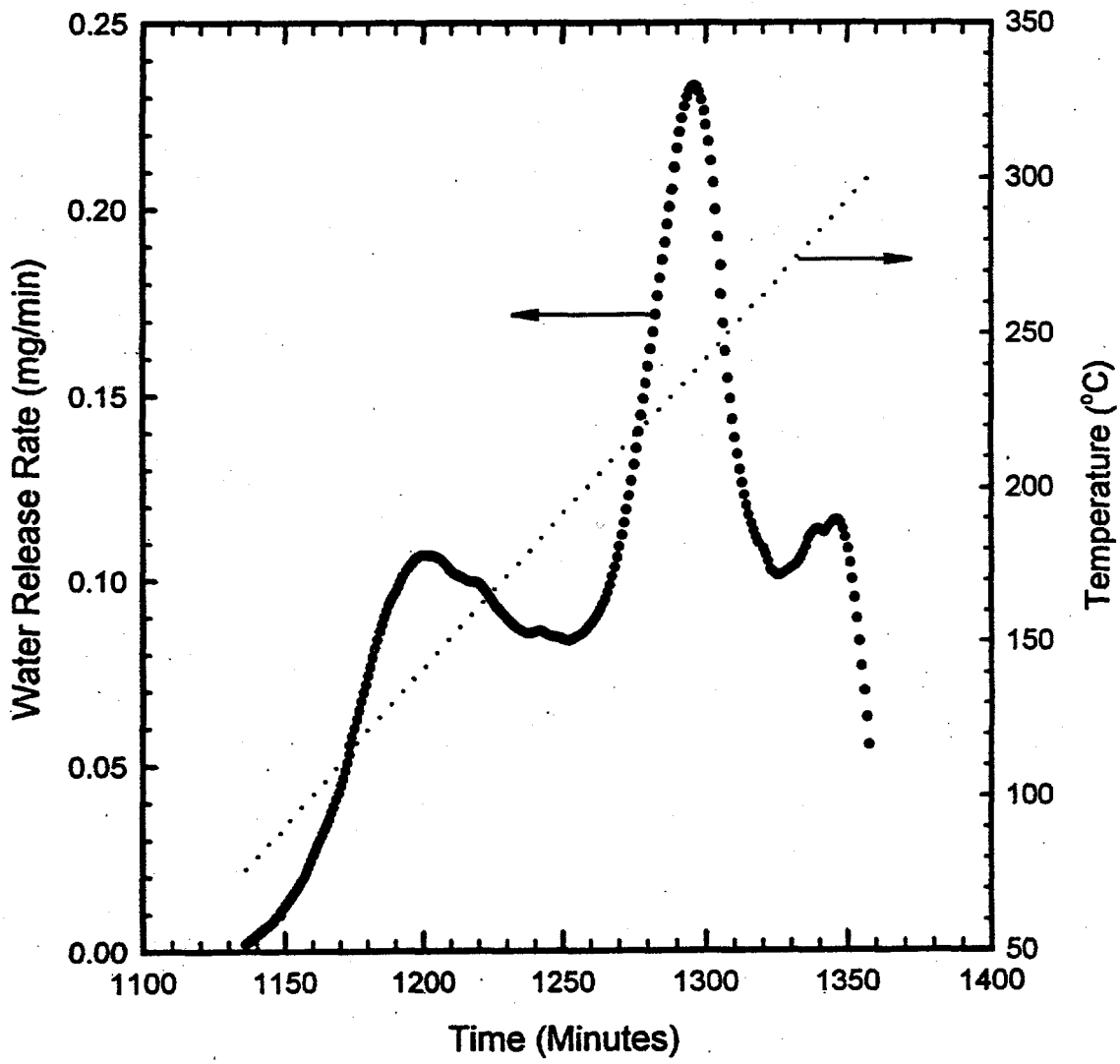

Figure A.9. Release Rate Curve for the Transient Temperature Data Between 75°C and 300°C for TGA Run 42, Indicating Three Different Peaks

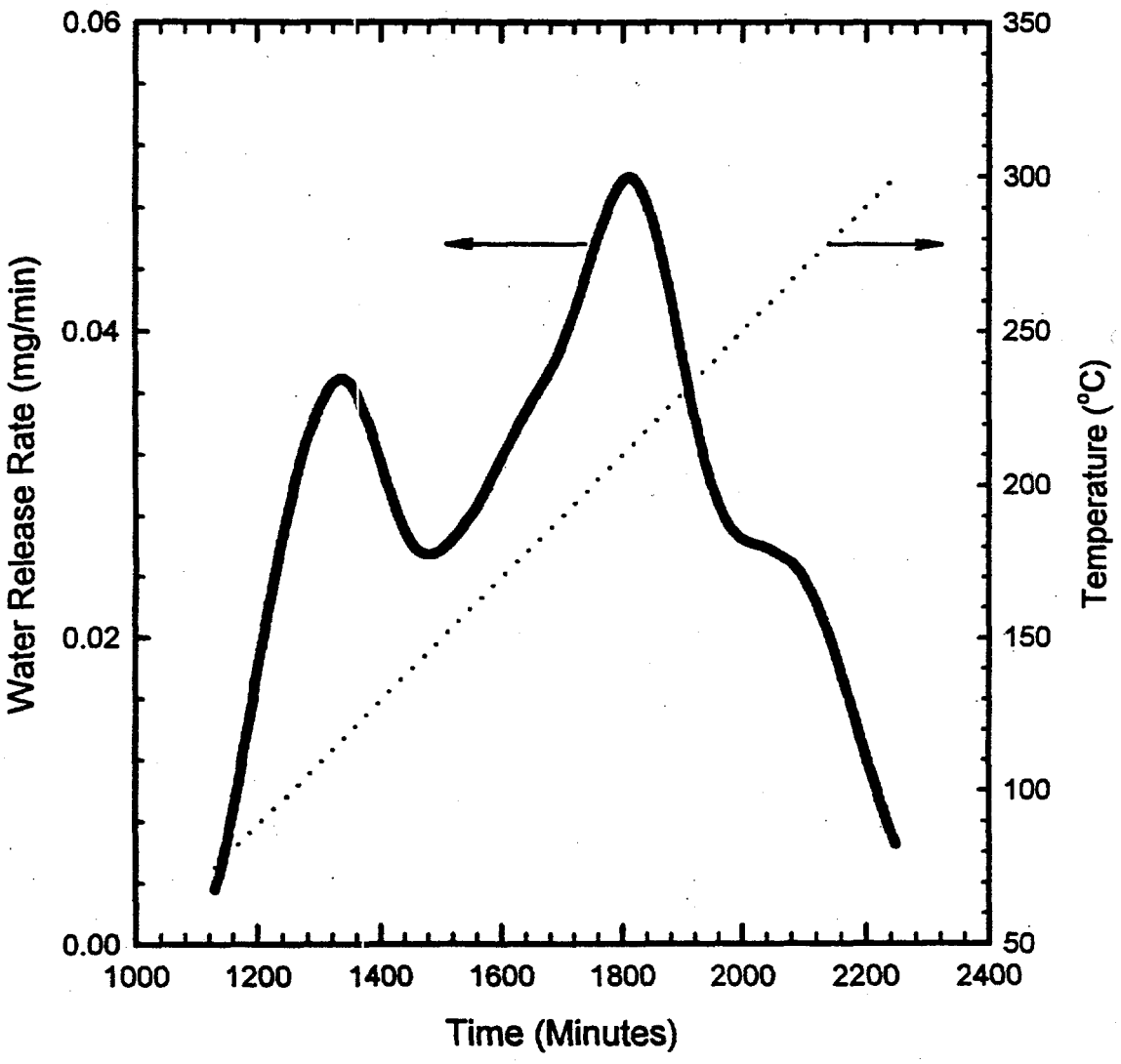

Figure A.10. Release Rate Curve for the Transient Temperature Data Between 75°C and 300°C for TGA Run 43, Indicating Three Different Peaks

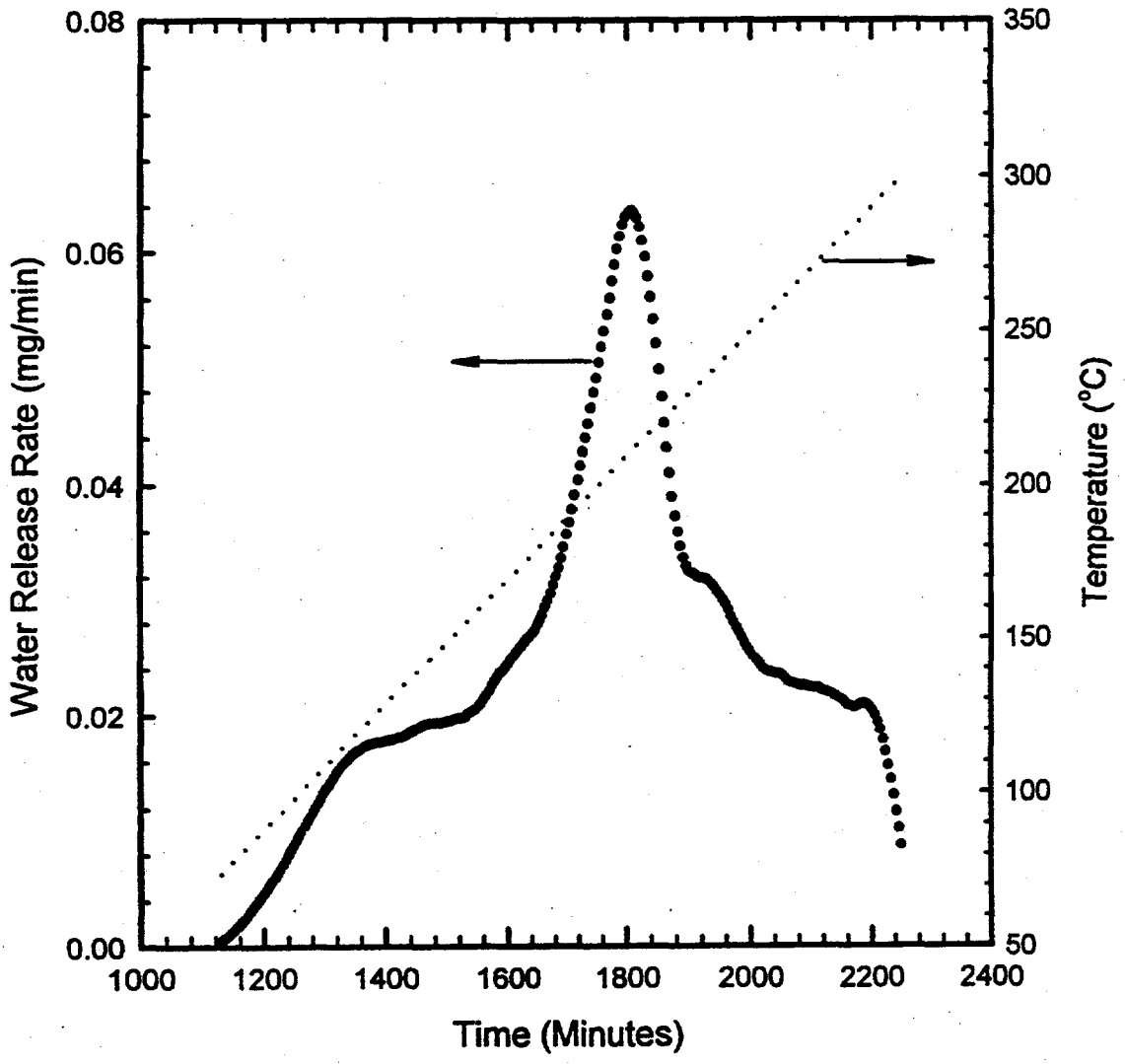

Figure A.11. Release Rate Curve for the Transient Temperature Data Between 75°C and 300°C for TGA Run 44, Indicating Three Different Peaks

Appendix B

XRD Spectra of K-East Canister Sludge Used in the Drying Studies

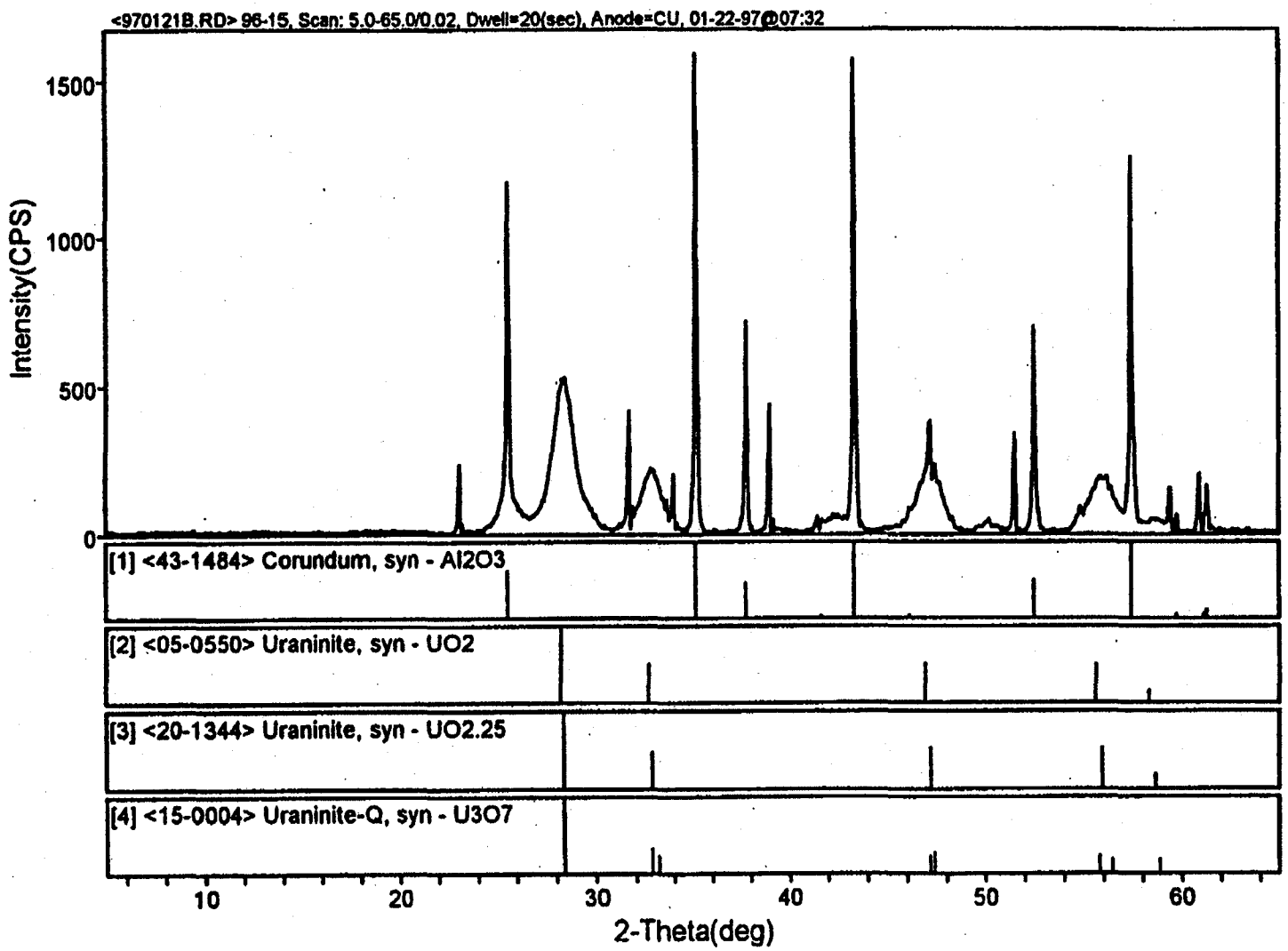

Figure B.1. XRD Spectrum of KE Canister Sludge 96-15

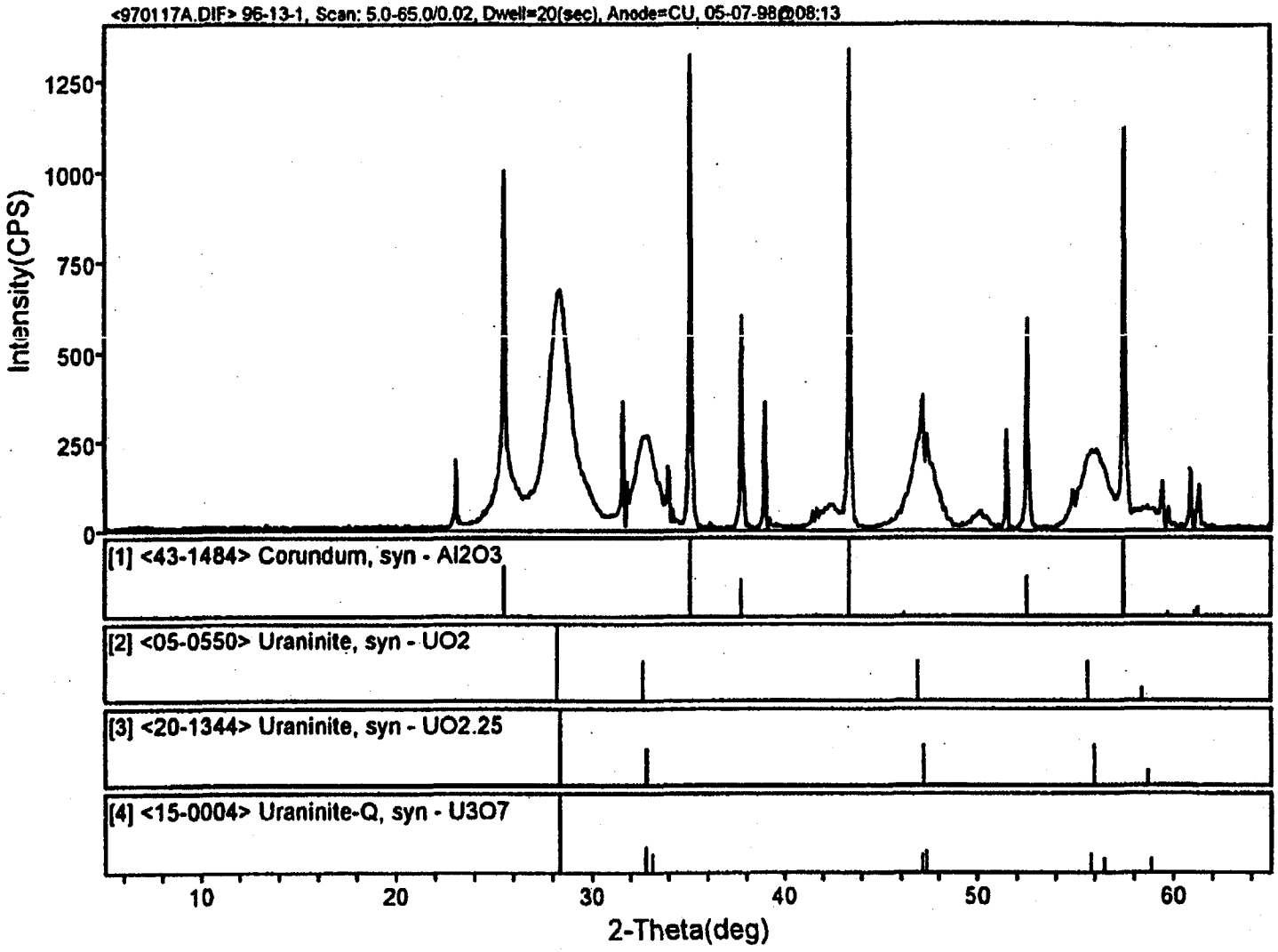

Figure B.2. XRD Spectrum of KE Canister Sludge 96-13

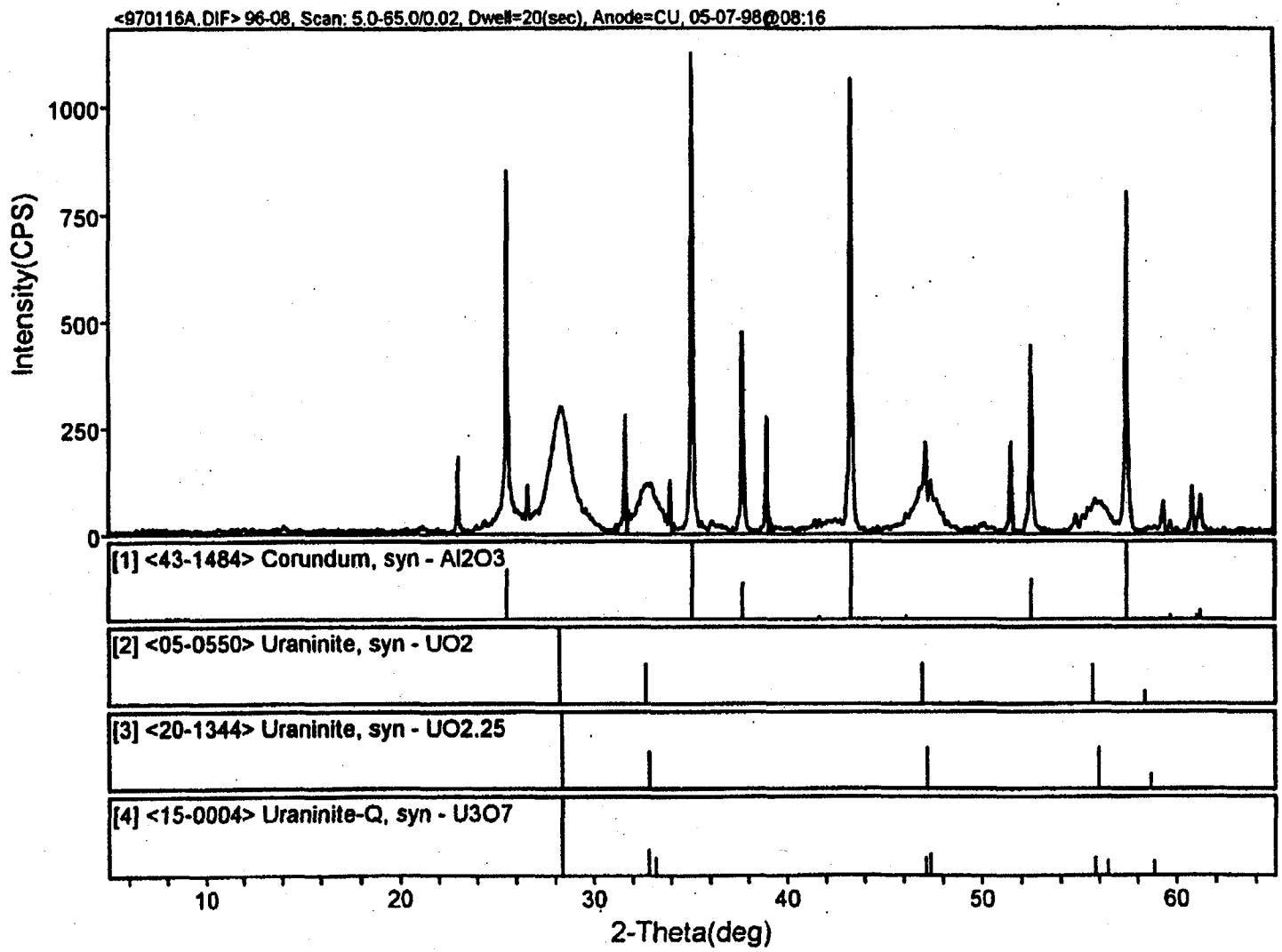

Figure B.3. XRD Spectrum of KE Canister Sludge 96-08

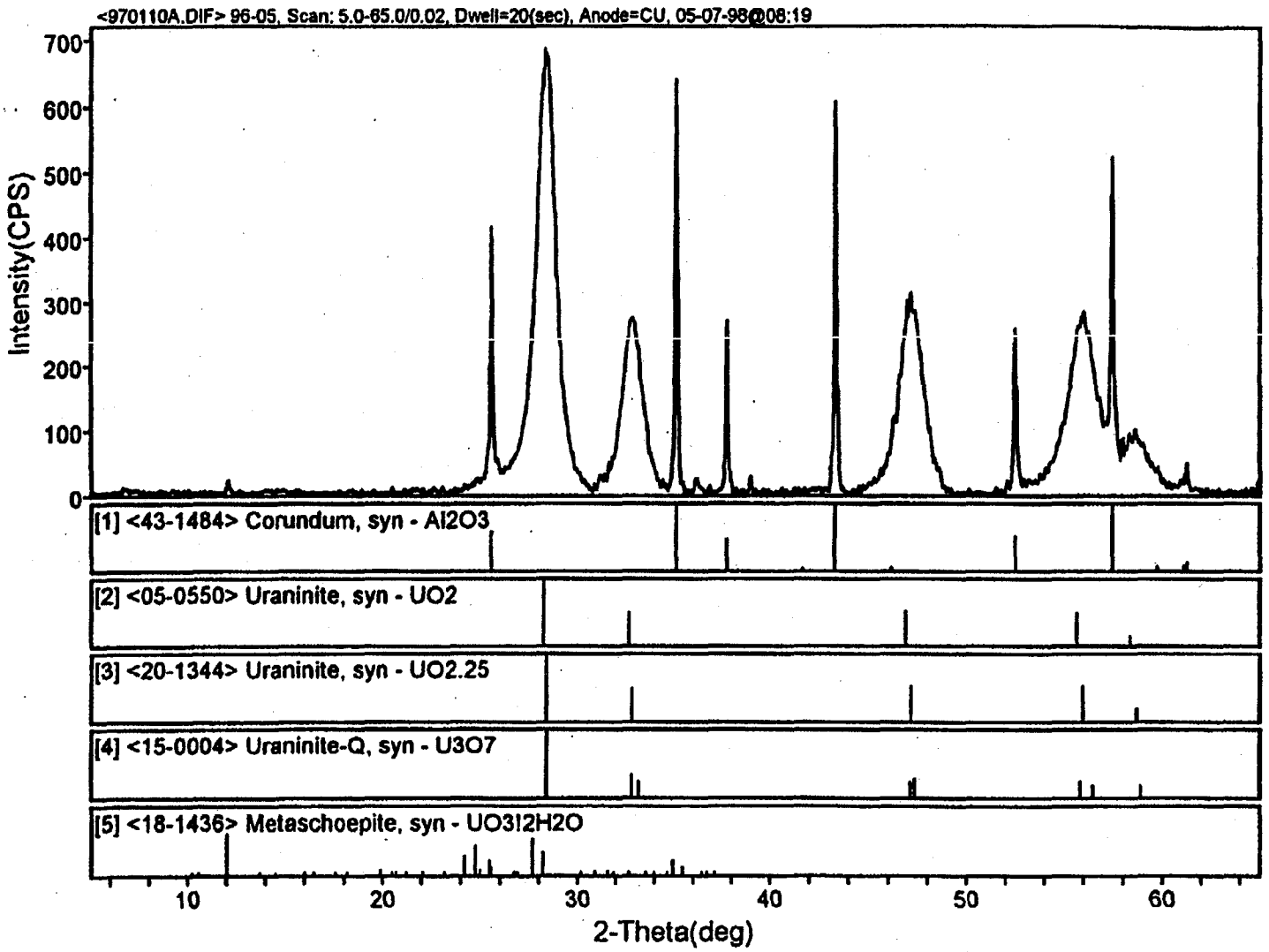

Figure B.4. XRD Spectrum of KE Canister Sludge 96-05

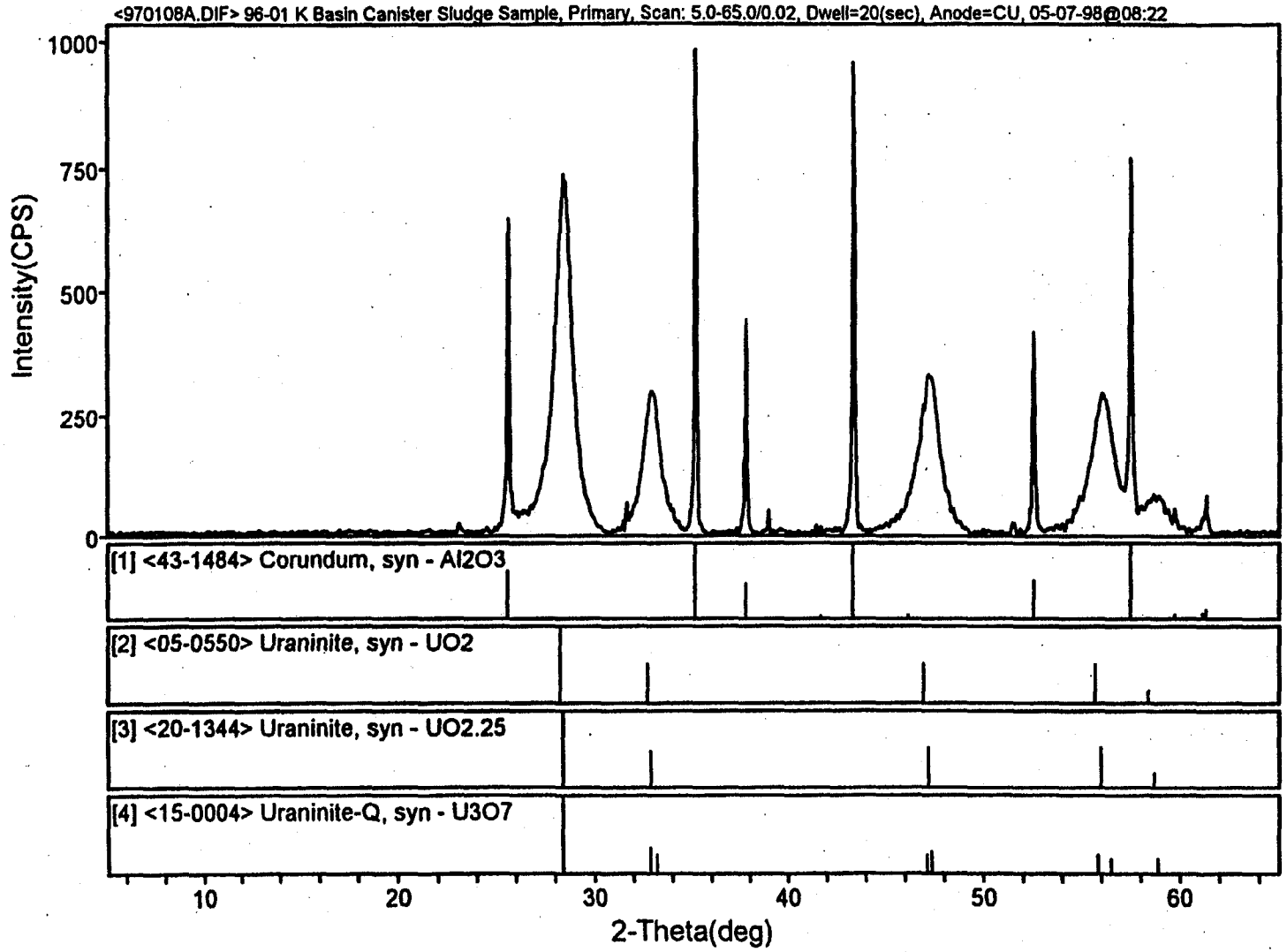

Figure B.5. XRD Spectrum of KE Canister Sludge 96-01

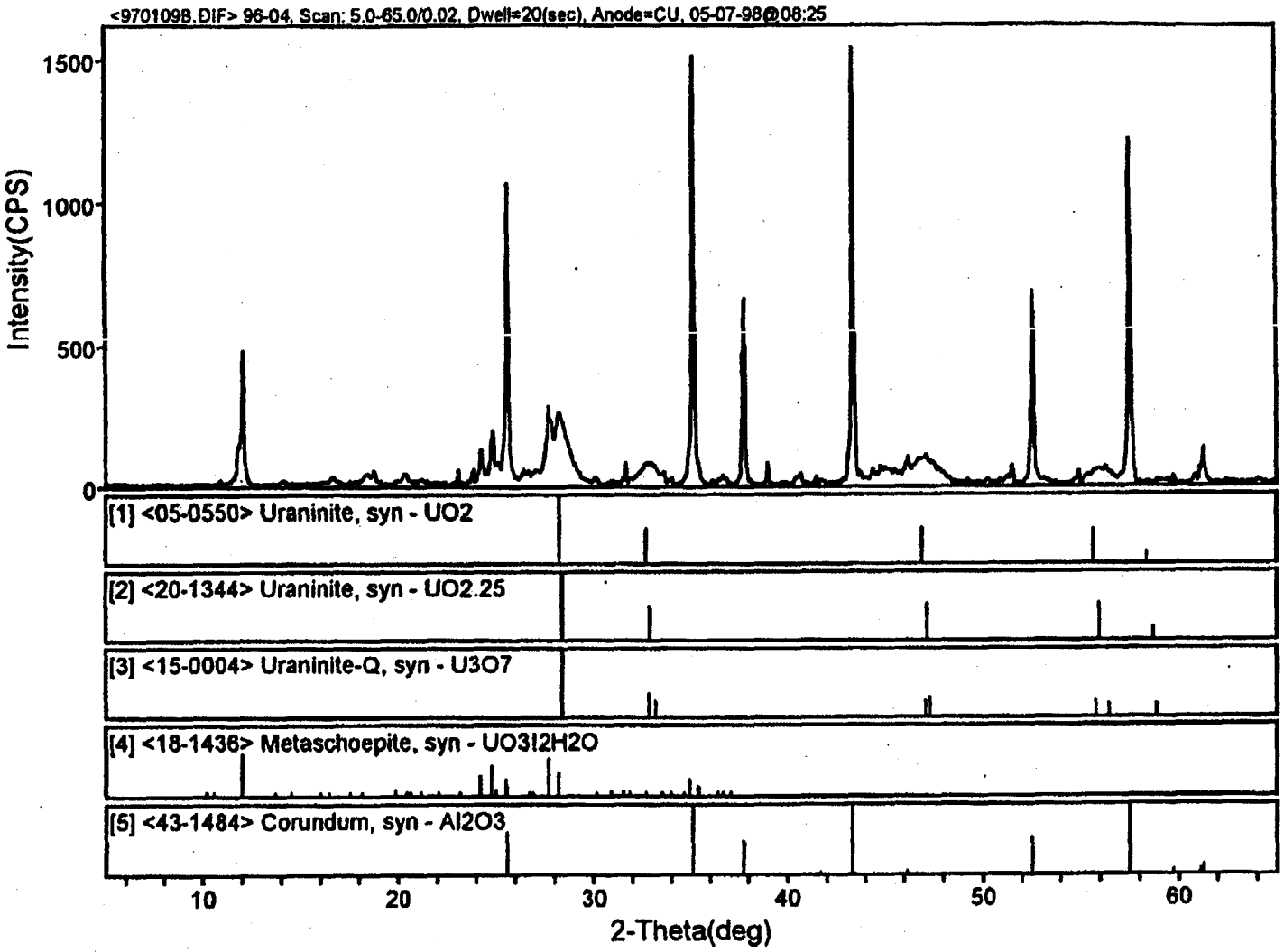

Figure B.6. XRD Spectrum of KE Canister Sludge 96-04/L

Distribution

No. of
Copies

OFFSITE

C. L. Bendixsen
Idaho National Engineering and
Environmental Laboratory
P.O. Box 1625
Mail Stop 3135
Idaho Falls, ID 83415

A. W. Conklin
Washington State Department of Health
Airdustrial Park
Building 5, Mail Stop LE-13
Olympia, WA 98504-0095

M. A. Ebner
Idaho National Engineering and
Environmental Laboratory
P.O. Box 1625
Mail Stop 3114
Idaho Falls, ID 83415

A. R. Griffith
U.S. Department of Energy, Headquarters
19901 Germantown Rd (EM-65)
Germantown, MD 20585-1290

T. J. Hull
U.S. Department of Energy, Headquarters
19901 Germantown Road (EH-34)
Germantown, MD 20874-1290

M. R. Louthan
Savannah River Technology Center
Materials Technology Center
Aiken, SC 29808

No. of
Copies

T. E. Madey
Rutgers University
Bldg. 3865
136 Freylinghuysen Rd
Piscataway, NJ 08854

B. K. Nelson
U.S. Department of Energy, Headquarters
19901 Germantown Road (EM-65)
Germantown, MD 20874-1290

R. G. Pahl, Jr.
Argonne National Laboratory
P. O. Box 2528
Idaho Falls, ID 83403

R. S. Rosen
Lawrence Livermore National Laboratory
20201 Century Blvd., 1ST Floor
Germantown, MD 20874

D. Silver
Washington State Department of Ecology
P.O. Box 47600
Olympia, WA 98504-7600

T. A. Thornton
Framatome Cogema Fuels
1180 Town Center Drive
Las Vegas, NV 89134

No. of Copies

ONSITE

7 DOE Richland Operations Office

D. Bryson	S7-41
R. M. Hiegel	S7-41
P. G. Loscoe	S7-41
C. R. Richins	K8-50
E. D. Sellers	S7-41
J-S. Shuen	S7-41
G. D. Trenchard	S7-41

23 Duke Engineering and Services, Hanford Inc.

R. B. Baker	H0-40
D. W. Bergmann	X3-79
S. A. Chastain	H0-40
D. R. Duncan	R3-86
J. R. Frederickson	R3-86
L. H. Goldmann	R3-86
S. L. Hecht	HO-40
J. J. Jernberg	X3-72
L. A. Lawrence (5)	H0-40
B. J. Makenas	H0-40
R. P. Omberg	H0-40
R. W. Rasmussen	X3-85
A. M. Segrest	R3-11
J. A. Swenson	R3-11
C. A. Thompson	R3-86
D. J. Trimble	H0-40
D. J. Watson	X3-79
J. H. Wicks, Jr.	X3-74
SNF Project Files	

3 Fluor Daniel Hanford

E. W. Gerber	R3-11
D. A. Smith	T4-13
M. J. Wiemers	R3-11

No. of Copies

3 Fluor Daniel Northwest

L. J. Garvin	R3-26
F. F. Huang	E6-15
G. A. Ritter	H0-40

7 Numatec Hanford Company

G. P. Chevrier	H5-25
T. Choho	R3-86
E. R. Cramer	H0-34
T. A. Flament	H5-25
J. J. Irwin	R3-86
C. R. Miska	R3-86
J. P. Sloughter	H5-49

SGN Eurisys Services Corp

A. L. Pajunen	R3-86

2 Technical Advisory Group

J. C. Devine	R3-11
R. F. Williams	R3-11

32 Pacific Northwest National Laboratory

J. Abrefah (5)	P7-27
J. P. Cowin	K8-88
S. R. Gano	K2-12
W. J. Gray	P7-27
B. D. Hanson	P7-27
G. S. Klinger	P7-22
D. K. Kreid	K7-80
J. M. Latkovich	K9-44
S. C. Marschman (10)	P7-27
B. M. Oliver	P7-22
T. M. Orlando	K8-88
J. C. Wiborg	K7-74
Information Release (7)	